Chapter 4

Snow and Ice in the Hydrosphere

Jan Seibert [1,2], Michal Jenicek [1,3], Matthias Huss [4,5] and Tracy Ewen [1]
[1] *Department of Geography, University of Zurich, Switzerland,* [2] *Department of Earth Sciences, Uppsala University, Uppsala, Sweden,* [3] *Department of Physical Geography and Geoecology, Faculty of Science, Charles University in Prague, Czech Republic,* [4] *Laboratory of Hydraulics, Hydrology and Glaciology (VAW), ETH, Zurich, Switzerland,* [5] *Department of Geosciences, University of Fribourg, Switzerland*

ABSTRACT
In large areas of the world, runoff and other hydrological variables are controlled by the spatial and temporal variation of the 0 °C isotherm, which is central for the temporal storage of precipitation as snow or ice. This storage is of crucial importance for the seasonal distribution of snow and ice melt, a major component of the movement of water in the global water cycle. This chapter provides an introduction to the role of snow and ice in the hydrosphere by discussing topics including snowpack characteristics, snow observation approaches, the energy balance of snow-covered areas, and modeling of snowmelt. Furthermore, the role of glaciers and glacial mass balances, including modeling glacier discharge, is discussed. Finally, an overview of the hydrology of snow- and ice-covered catchments is given, and the influence of snow, glaciers, river ice, and frozen soils on discharge is discussed.

4.1 INTRODUCTION

Snow and ice are important components of the hydrosphere, and many processes related to snow and ice are dominated by the important threshold behavior caused by the large amount of energy, which is released or consumed during the phase change between liquid and frozen water. In the Northern Hemisphere, about one-quarter of the area experiences mean annual temperatures that are below 0 °C, and for more than half of the area, temperatures are below 0 °C during at least one month of the year (Brown and Goodison, 2005; Davison and Pietroniro, 2005). Hence, a permanent or seasonal snow cover exists in large parts of the world, even if the snow cover extent in the Southern Hemisphere is much less (~2% of that in the Northern Hemisphere). The annual snowfall

Snow and Ice-Related Hazards, Risks, and Disasters. http://dx.doi.org/10.1016/B978-0-12-394849-6.00004-4

fraction increases with elevation and latitude, where the amount of solar energy varies significantly over the year. Overall, the climate determines where snowfall typically occurs, and drivers at the global, regional, and local scales all play a role. The characteristically small difference in temperature that determines whether precipitation falls as rain or snow can have large effects on ecosystems. In regions where there is either a permanent or seasonal snow cover, snow significantly influences all aspects of the cryosphere and many environmental variables, as well as social and economic patterns.

The existence of snow cover on the ground directly changes the partitioning of the incoming energy. Snow has a high albedo, which means that a large fraction of the incoming solar energy is reflected back into the atmosphere. The albedo of new snow can be up to about 0.9 and decreases to about 0.5 as snow ages, whereas typical values for areas without snow cover are 0.1–0.3 (Table 4.1). This difference explains the observation that mean air temperatures are significantly lower ($\sim 5\,^{\circ}C$) if the ground is covered by snow, which implies that there is a positive feedback that can enhance the accumulation of snow in early winter and maintain the snowpack longer into late spring and summer.

Snow also has a high insulation capacity, which means that energy fluxes between the atmosphere and the ground are significantly reduced by snow. It has, for instance, been observed that seasonal soil freezes to deeper depths if there is no snow present compared to the situation with an insulating snow cover (Hayashi, 2013). Wintertime snowpack also acts as insulation for the local environment, providing an insulating cover for vegetation and hibernating animals.

TABLE 4.1 Albedo of Various Surfaces for Short-Wave Radiation

Surface	Typical Range in Albedo (–)
New snow	0.80–0.90
Old snow	0.60–0.80
Melting snow (porous → fine grained)	0.40–0.60
Snow ice	0.30–0.55
Coniferous forest with snow	0.25–0.35
Green forest	0.10–0.20
Bare soils	0.10–0.30
Water	0.05–0.15

Based on Hendriks, 2010; Maidment, 1992.

The spatial and temporal variation of the 0 °C isotherm is central for the temporal storage of precipitation as snow or ice. This storage is of crucial importance for the seasonal distribution of snow and ice melt, a major component of the movement of water in the global water cycle. In many areas, snow and ice melt is the main contribution to annual river runoff and can affect water supply, hydropower production, agricultural irrigation, and transportation. In extreme cases, large snowmelt rates, sometimes combined with heavy springtime rainfall, may lead to disastrous flooding. Rapid snowmelt can also trigger landslides and mass wasting of hill slopes. Too little snowmelt, on the other hand, can lead to low river flows in summer, or even drought, which can have significant economic, environmental, and ecological consequences. Especially in many arid regions of the world, the temporal storage of snow in nearby mountainous regions is of critical importance for water supply.

In this chapter, we provide an overview of the role of snow and ice in the water cycle. In the following section on snow accumulation and snowpack properties, we address topics including snowpack characteristics, snow observation approaches, energy balance of snow-covered areas, and modeling of snowmelt. In the section that follows, we discuss glaciers and glacial mass balance, including modeling glacier discharge. In the final section, an overview of the hydrology of snow- and ice-covered catchments is given, and the influence of snow, glaciers, river ice, and frozen soils on discharge is discussed. The present chapter thus mainly provides a background to the other chapters in this volume, which discuss the different aspects of snow- and ice-related natural hazards.

4.2 SNOW ACCUMULATION AND MELT

4.2.1 Snowpack Description

A snowpack can be described in many different ways. Although snow depths can be easily measured, the snow water equivalent (S_{WE} in mm) is the more relevant property of a snowpack for most snow hydrological questions since the S_{WE} is the water content in snow that directly contributes to runoff. The S_{WE} is defined as the amount of liquid water that would be obtained upon complete melting of the snowpack per unit ground surface area. S_{WE} (mm), snow depth (d (m)), snow density (ρ_s (kg m^{-3})), and water density ($\rho_w = \sim$1,000 kg m^{-3}) are directly related (Eqn (4.1)). The density of snow can vary considerably (Table 4.2) (DeWalle and Rango, 2008; Fierz et al., 2009; Maidment, 1992; Singh and Singh, 2001). New snow generally has the lowest densities with about 100 kg m^{-3}, and densities increase with aging snow due to metamorphism to about 350–400 kg m^{-3} for dry old snow and up to 500 kg m^{-3} for wet old snow. Firn, snow that has not melted during the past summer, has densities typically ranging from 550 to 800 kg m^{-3}.

TABLE 4.2 Typical Snow Density for Different Snow Types

Snow Type	Density (kg m^{-3})
New snow (immediately after falling in calm conditions and at very low temperature)	10–30
New snow (immediately after falling in calm conditions)	50–70
Wet new snow	100–200
Settled snow	200–300
Depth hoar	200–300
Wind packed snow	350–400
Wet snow	350–500
Firn	500–830
Glacier ice	850–917

Based on DeWalle and Rango, 2008; Fierz et al., 2009; Maidment, 1992; Singh and Singh, 2001.

$$S_{WE} = 1000d\frac{\rho_s}{\rho_w}. \tag{4.1}$$

Different types of precipitation also impact the density of the snowpack. These include the type of snow (wet or dry), graupel, sleet (or ice pellets), freezing rain, freezing drizzle, rain, and drizzle. The type of snow crystal, determined during formation by the temperature and moisture content of the atmosphere, also affects the density of the snowpack. The most complex crystal structures tend to form light, low-density snowpacks due to the large spacing in between their branches. Smaller crystals such as plate crystals, needles, and columns, tend to form heavier, high-density snowpacks because they pack together very efficiently, leaving little space for air pockets in between. Changes in snowpack density due to the increase in the pressure of the top layers are caused by the mass of newly fallen snow on the older snow. The increase in the snow density causes the increase in the thermal conductivity of the snowpack. For a further discussion of snow density related to snow microstructure, see (Arenson et al., 2014) (this volume).

At the catchment scale, the amount of snow stored in a catchment is determined by the spatial distribution of S_{WE}, which is largely controlled by the spatial distribution of snow depths. Another important variable is the fractional snow cover. Snow depletion curves describe the S_{WE} as a function of fractional snow cover and are important for forecasting seasonal runoff during periods with a gradual decrease in snow cover. In alpine areas, the curves are commonly s-shaped, reflecting the area–elevation curve, which is typically

steep in the low and higher elevations and flatter in the middle elevations (Seidel and Martinec, 2010).

4.2.2 Snow Accumulation

4.2.2.1 Spatial Distribution of Snow

Large-scale variations of snow accumulation are controlled by temperature, which in turn is related to elevation and latitude (Essery, 2003; Jost et al., 2007) and exposition, whereas at smaller scales, the effects of topography on snow redistribution and of forests on snow accumulation and snowmelt can be pronounced. The forest affects snow interception, wind speed, and the density of the snowpack, depending mainly on the type of forest (i.e., coniferous, deciduous, or mixed species), forest age, and canopy cover. The role of the forest is also important during the melting period because it reduces the amount of short-wave solar radiation reaching the surface and thus snowmelt rates (Holko et al., 2009; Jeníček et al., 2012; Jost et al., 2007, 2009; López-Moreno et al., 2008).

Stähli and Gustafsson (2006) evaluated the effect of forests on snow accumulation in a small prealpine catchment in Switzerland. They found that as a long-term average, annual maximum S_{WE} was about 50 percent less in the forest than in open areas. The importance of this effect decreased with increasing snowfall. They also found that the variability of S_{WE} increased throughout the winter season and could be explained by varying snow accumulation and melt at different altitudes and exposures. Similar findings were obtained in several paired catchment studies after clear-cutting. For a catchment in Northern Sweden, for instance, it was observed that the S_{WE} increased after clear-cutting by about 30 percent at the end of the accumulation period, snowmelt occurred earlier and spring flood runoff increased significantly in some years (Schelker et al., 2013). Overall, clear-cutting increases the snowpack and the S_{WE} directly since snow is no longer intercepted by the vegetation canopy. Clear-cutting will also have a local effect on the wintertime energy budget through an increase in albedo.

4.2.2.2 Snow Observations

Snowfall can be measured by precipitation gauges in the same way as rainfall, but the errors due to wind effects are commonly significant and systematic underestimates of $\geq$50 percent have been reported (Rasmussen et al., 2012; Sevruk et al., 2009). Adaptations of precipitation gauges to improve snowfall measurements include heated gauges, which melt the snow and allow the S_{WE} of the snowfall to be measured directly, or gauges with large inverted cone shields that can improve measurements in open, windy areas. Without heating, snowfall commonly accumulates on top of the gauge, resulting in erroneous measurements (Figure 4.1). Unlike rainfall, snow remains on the ground and can also be measured in situ.

FIGURE 4.1 Nonfunctioning precipitation gauge after heavy snowfall (Mumsarby/Dannemora, Sweden).

Snow depth, either the entire snowpack or the amount of newly fallen snow, is generally measured using a snow stake, which is simply a height measurement taken at the snow surface with the zero point either at the ground surface or last snow layer. Snow depth can also be measured using automatic sensors that usually apply an ultrasonic beam reflecting from the ground level. For low-cost measurements carried out in many different localities, time-lapse photography can be used (e.g., Garvelmann et al., 2013). This solution enables not only snow depth to be measured but it also allows information about site conditions during the observing period to be recorded, such as rain-on-snow events, cloudiness, and snow interception on the canopy.

The S_{WE} can be measured directly by taking a snow core with a snow tube, and then weighing the snow and dividing by the area of the opening of the snow tube. As an alternative, the S_{WE} can be computed from measurements of snowpack depth (d (m)) and estimates of snow density (ρ_s) using Eqn (4.1) and the density of liquid water ($\sim$1,000 kg m^{-3}). Because snow depth generally varies spatially more than snow density does, and is also easier to measure, it is usually a good strategy to measure snow depth at a frequency at least 10 times greater than snow density. Statistical estimation methods of snow density and its evolution during winter can be used in cases where only snow depth data are available (Jonas et al., 2009). Such approaches generally give similar results to more complex physically based modeling of S_{WE} (Bavera et al., 2014).

For continuous S_{WE} measurements, a snow pillow or snow scales are commonly used (Figure 4.2). Such observations are based on measuring the mass of the snow lying on the installed pillow or sensor plate with a specific area (usually $\sim 9\ m^2$). Another way of measuring S_{WE} in situ is a snow permittivity measurement of the snowpack (Egli et al., 2009). This measurement is based on measuring the dielectric constant of three main components of the snowpack: ice, water, and air. The measurement is carried out along a ribbon placed in the snowpack (usually placed parallel or diagonal to the

FIGURE 4.2 Climate station with snow scales in Modrava, Czech Republic (left), and snow pit close to the Furka Pass, Switzerland (right). *Photograph: M. Jenicek.*

ground). With this system, it is possible to measure the S_{WE}, snow density, and liquid water content.

For mapping S_{WE} over larger areas, promising results have been achieved using ground-based or airborne ground-penetrating radar (Lundberg et al., 2006; Sold et al., 2013). An alternative is the measurement of gamma radiation from the earth (Peck et al., 1971). The method is based on the attenuation of natural gamma radiation by the water accumulated in the snowpack with a detector fixed either a few meters from the ground surface or read from an aircraft. Gamma radiation is then measured over time with and without snow cover. A more recent technique is the highly accurate remote sensing of the snowpack on the ground and on glaciers using laser scanners (Egli et al., 2012; Grünewald et al., 2010; Prokop, 2008; Sold et al., 2013). Sensors can be placed in the aircraft (light detection and ranging, LIDAR) or can be used as a terrestrial device placed on the tripod (terrestrial laser scanning). Due to their construction and method of use, scanners have enabled the remote sensing of areas that are impossible to measure directly, for example, distant locations or steep slopes prone to ice or snow avalanches or rock falls (Egli et al., 2012; Grünewald et al., 2010). Present sensors are highly accurate (<1 cm both horizontally and vertically). However, not all sensors can be used for snow sensing due to the reflection properties of the snow cover (Prokop, 2008). Because of the high acquisition cost of laser scanners, a laser range finder is in some cases used to determine the snow depth (Hood and Hayashi, 2010). The disadvantages of these devices are mainly (1) poorer resolution of the snow depth grid; (2) generally only a small area can be covered from one location; and (3) measurements take more time than with a terrestrial laser scanner. Despite these disadvantages,

the device is highly portable and a potentially improved alternative to expensive laser scans.

In recent years, much progress has been made using remote airborne and space-borne sensing methods to determine snow characteristics (Molotch and Margulis, 2008; Tait, 1998; Vander Jagt et al., 2013). These methods provide information about snow cover, generally for large areas, and basically on-line. Methods for remotely determining the S_{WE} based on the repeated monitoring of snow cover area (SCA) have been developed (Farinotti et al., 2010; Molotch and Margulis, 2008). The SCA can be measured by both optical and radar instruments. Radar is also suitable for observations of other parameters such as the amount of liquid water content (Storvold et al., 2006), and passive microwave sensors can also be used to derive S_{WE} (Molotch and Margulis, 2008; Tait, 1998).

4.2.3 Snow Redistribution, Metamorphism, and Ripening Process

4.2.3.1 Snow Redistribution by Wind

Snow transport, or the deposition of falling snow, is controlled by the wind field of the surface boundary layer, which is modified (in speed and direction) by local surface topography (Lehning et al., 2008). Variability in the wind field ultimately causes snow to be nonuniformly distributed or redistributed over the landscape. The spatial variation of S_{WE} is commonly strongly influenced by the effects of topography on snow redistribution and the timing of the snow disappearance is in turn controlled by this redistribution, in addition to differences in melt rates (Anderton et al., 2004) (Figure 4.3). The spatial redistribution of snow affects the basin-averaged snowmelt to different degrees; the

FIGURE 4.3 Spatial distribution of snow as a result of varying snow accumulation and melt and snow redistribution (Furkapass, Switzerland, June 2013). Snow on the south-facing side of the valley had already melted, whereas on the north-facing side, snow was still present in areas that had gained snow due to snow redistribution.

effects of snow redistribution were found to be very important for Reynolds Creek (Idaho, US; Luce et al., 1998), whereas only local effects were reported for an area in the German Alps (Bernhardt et al., 2012). For Reynolds Creek, the spatial redistribution of snow in drifts sustained streamflow later into the spring and summer compared to a more uniform snowpack.

4.2.3.2 Snow Metamorphism

The process of snow crystal metamorphism begins immediately after snowpack accumulation on the ground. In nature, most crystal changes are related to pressure and temperature changes in the snowpack (DeWalle and Rango, 2008). The three main types of snowpack metamorphism are briefly discussed below (see the Chapter by Arenson et al. (2014) for a discussion of metamorphism in the context of snow microstructure).

Equitemperature metamorphism is based on the migration of vapor from convex to concave ice surfaces because of higher vapor pressure on convex surfaces of the crystals than on concave surfaces. Snow crystals became more rounded due to this process. More rounded crystals increase snowpack stability due to their higher compaction ability and thus reduce the risk of avalanches.

Temperature-gradient metamorphism occurs as a result of changes in snowpack temperature and is the most important premelt densification process for the snowpack. The physical principle is based on the higher vapor pressure in a warmer snowpack than in a cooler snowpack. This gradient causes an upward migration of water vapor within the snowpack, from the warmer ground surface to the cooler snow surface. This process causes the formation of a new layer with large faceted crystals (depth hoar) that are poorly connected to each other, and thus, snowpack stability on the slope is lower and more prone to avalanches (e.g., Fierz et al., 2009). This depth hoar layer can be recognized only by snow pit analysis, which is infrequently carried out due to the time and effort required, and it thus represents a potential danger.

Melt-freeze metamorphism is typical during the spring period when air and snowpack temperatures increase due to the higher solar radiation. Snow on the surface of the snowpack tends to melt first, typically the small snow grains because they have lower melt temperatures compared to large snow grains. The melted snow can trickle into the colder middle portion of the snowpack where it refreezes and leads to the formation of a well-connected, large-grained snowpack. A specific amount of liquid water is generally present in the snowpack before snowmelt; typically from 2 to 5 percent with a maximum of 10 percent (e.g., Fierz et al., 2009; Techel and Pielmeier, 2011). A higher portion of liquid water can lead to the specific type of snow and water movement called slush flow that commonly also activates a top soil layer (Eckerstorfer and Christiansen, 2012). Melt-freeze metamorphism generally increases snowpack stability. On the other hand, the avalanche danger increases with an increase in the volume of liquid water stored in the snowpack.

For an in-depth discussion on snowpack stability and avalanches, the reader is referred to Schweizer et al. (2014) (this volume).

4.2.4 Snowpack Development

In regions where there is a seasonal snowpack, the snowpack develops over the course of the season starting with an accumulation phase, when precipitation falling as snow accumulates, increasing the S_{WE} until the melt period begins with an increased input of solar radiation. At first, the melt is characterized by a warming phase, when the average snowpack temperature increases more or less steadily until the snowpack becomes isothermal, that is, when the temperature over the snow profile reaches 0 °C. At this point, melting within the snowpack is possible and marks the beginning of the ripening phase. The melt within the snowpack is retained until the liquid, water-holding capacity is exceeded. Once exceeded, any further input of energy (from warmer air and/or soil and/or liquid precipitation) gained by the snowpack will then be used for phase changes from solid to liquid, producing more melt. The output phase begins when water output occurs at the base of the snowpack. It is important to note that a snowpack, as a porous medium, can store considerable amounts of liquid water. As a rule of thumb, snow can hold up to about 10 percent of the snowpack S_{WE} by capillary forces against gravitation.

4.2.4.1 Cold Content

The cold content of a snowpack is the total heat that is necessary to warm the snowpack to 0 °C over the entire vertical profile and can be expressed as the amount of liquid water (in (m)), which must be frozen in the snowpack to warm the snowpack to isothermal conditions (DeWalle and Rango, 2008). This variable of the energy state of a snowpack is important for snowmelt processes and their modeling and can be calculated as

$$C_C = \frac{\rho_s \cdot c_i \cdot d \cdot (273.16 - T_s)}{\rho_w \cdot L_f}, \tag{4.2}$$

where C_C (m) is the snowpack cold content, ρ_s is the snowpack density (kg m^{-3}), c_i is the specific heat of ice (J kg^{-1} K^{-1}), d is the snowpack depth (m), T_s is the snowpack temperature (K), ρ_w is the water density (kg m^{-3}), and L_f is the latent heat of fusion (J kg^{-1}).

Cold content is commonly used by hydrologists when simulating snowmelt runoff. Generally, it can be calculated for the whole profile or for specific snowpack layers, which is useful for modeling avalanches. The evolution of the snowpack and snowpack temperatures in specific layers can be used to calculate the cold content over the accumulation and melt periods (Figure 4.4).

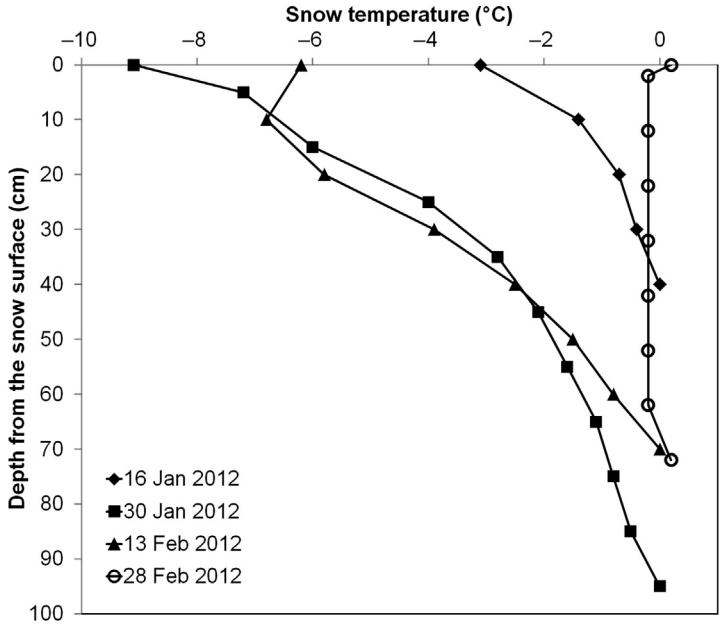

FIGURE 4.4 Snow-temperature evolution in a snow pit during the winter of 2011/2012; Krušné Mountains, Czech Republic. January 16 and January 30, 2012, represent typical winter conditions with low air temperatures. The third date, February 13, 2012, represents the beginning of spring warming (note the snow-temperature inversion in the top 10 cm of the snowpack). February 28, 2012, represents isothermal conditions in the snowpack during snowmelt. *Data from the Charles University in Prague, Faculty of Science.*

4.2.5 Snowmelt

4.2.5.1 Energy Balance

The development of the snowpack depends on the amount of energy available to the snowpack for melting snow that can be expressed in terms of the snowmelt energy balance. The energy balance of the snowpack represents the basic approach to snowmelt modeling and calculates all heat fluxes between the atmosphere, snow, and soil (Figure 4.5). The snowmelt energy balance can be defined by

$$Q_m = Q_{ns} + Q_{nl} + Q_h + Q_e + Q_p + Q_g + Q_i, \tag{4.3}$$

where all Q refer to heat fluxes (W m^{-2}). Q_m is the total heat flux (positive or negative) available for snow melting, Q_{ns} is the heat flux due to short-wave radiation, Q_{nl} is the heat flux due to long-wave radiation, Q_h is the sensible heat flux, Q_e is the latent heat flux caused by water phase changes, Q_p is the heat supplied by precipitation, Q_g is the heat supplied by the ground, and Q_i is the change in the internal energy of the snowpack.

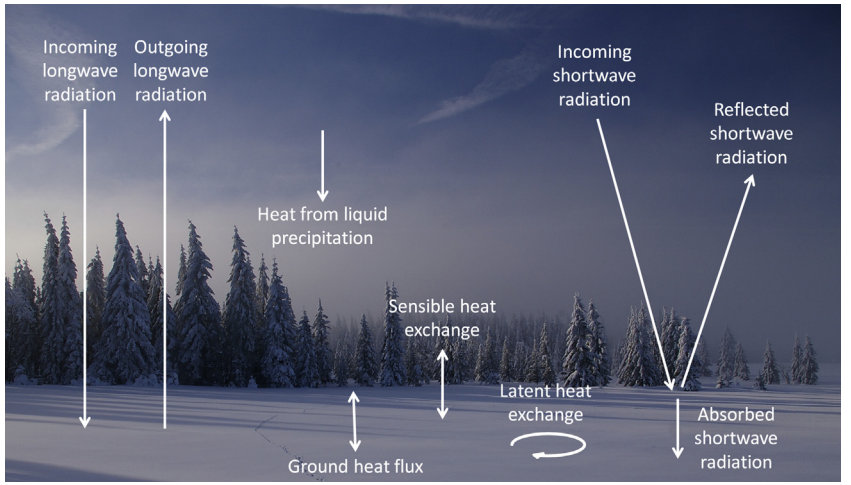

FIGURE 4.5 Energy balance of the snowpack. The arrows represent individual heat fluxes and interactions between the atmosphere, snow, and soil environments. *Photograph: M. Jenicek.*

The short-wave and long-wave radiation balance of the snowpack Q_{nr} can be computed according to

$$Q_{nr} = (1 - \alpha) \cdot S_i + (L_i - L_o), \tag{4.4}$$

where Q_{nr} (W m^{-2}) is the total radiation (sum of Q_{ns} and Q_{nr}), α (−) is the albedo, L_i is the incoming long-wave radiation, L_o is the outgoing long-wave radiation, and S_i is the incoming short-wave radiation (all in W m^{-2}) (Singh and Singh, 2001). The amount of short-wave radiation absorbed by snow depends mainly on latitude, season (sun inclination), atmospheric diffusion, slope, aspect, and obstacles with shadow effects like forest cover (see also Figure 4.6).

Long-wave radiation (in the range of 6.8−100 μm) is both incoming (from the atmosphere, surrounding terrain, and vegetation) and outgoing from the snow surface (Singh and Singh, 2001). The radiation from the surface is largely absorbed by the atmosphere, largely by absorption from carbon dioxide and water vapor.

A convective sensible heat transfer between the air and the snow is driven by differences between air and snowpack temperatures. The amount and the direction of the heat flux is given by

$$Q_h = \rho_a \cdot C_{pa} \cdot (T_a - T_s / r_h), \tag{4.5}$$

where ρ_a is the density of air (kg m^{-3}), C_{pa}, the specific heat of air at constant pressure (1,010 J kg^{-1} °C^{-1}), T_a and T_s (°C) are the air and snow surface temperatures, respectively, and r_h is a term to describe the resistance to a heat flux between the snow surface and the overlying air (s m^{-1}), which is a function of surface roughness and wind speed. For the sensible heat flux, large

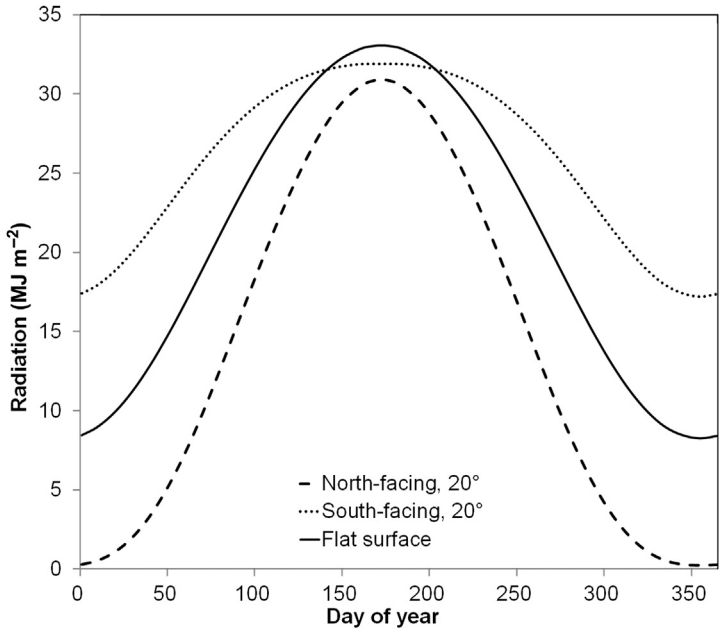

FIGURE 4.6 Daily potential solar irradiation for north and south-facing slopes at an inclination of 20° and a flat surface as a function of day of the year (i.e., Julian date) at a latitude of 45°N. The calculation considers clear sky conditions. *Based on the method presented in Dingman (2008).*

differences between the snow surface and air in spring and early summer cause an energy gain of the snowpack. However, the snowpack temperature is commonly higher than the air temperature during spring nights, and this situation represents a snowpack energy loss.

The latent heat transfer represents the transfer of water vapor between the atmosphere and the snowpack due to water phase changes, namely, evaporation and sublimation. The water vapor flux and its direction are determined by the vapor-pressure gradient and the intensity of the turbulence. Evaporation and the sublimation from the snow represent a snowpack energy loss; condensation and the deposition of the water vapor on the snow surface represent a snowpack energy gain. The latent heat flux is given by

$$Q_e = L_v \cdot (\rho_{va} - \rho_{vs})/r_e, \tag{4.6}$$

where L_v is the latent heat of vaporization (2.47×10^6 J kg^{-1}), ρ_{va} and ρ_{vs} are the vapor densities of air and snow surfaces, respectively (kg m^{-3}), and r_e (s m^{-1}) is a term to describe the resistance to water vapor transport between the air and snow surface, which is a function of surface roughness and wind speed.

Liquid precipitation on snow, known as rain-on-snow events, represents an additional heat flux into the snowpack that is caused by the higher temperature of the precipitation compared to the temperature of the snow. The heat

supplied to the snowpack equals the difference of snow energy before and after precipitation, once temperature equilibrium is reached. Equation (4.7) expresses the daily amount of transferred energy Q_p (kJ m^{-2} d^{-1}) depending on the precipitation P_r (mm d^{-1}) and the temperature difference (Singh and Singh, 2001),

$$Q_p = \frac{\rho_w \cdot C_p \cdot (T_r - T_s) \cdot P_r}{1000} + \rho_w \cdot L_f \cdot P_r, \tag{4.7}$$

where ρ_w refers to the water density ($\sim$1000 kg m^{-3}), C_p refers to the specific heat capacity of water (4.20 kJ kg^{-1} °C^{-1}), T_r is the temperature of liquid precipitation, T_s is the temperature of the snowpack (both in (°C)), and L_f is the latent heat of fusion (334 kJ kg^{-1}). Equation (4.7) is also valid when the snowpack is below freezing, and the rain freezes within the snowpack ($L_f > 0$).

The total amount of heat from the precipitation is generally quite low in comparison with other heat sources. However, precipitation heat input becomes more important when shorter time steps (less than one day) are considered. For example, a daily precipitation of $P_r = 30$ mm, rain temperature of $T_r = 10$ °C, and snow temperature of $T_s = 0$ °C results in a total heat input of 1,260 kJ m^{-2} d^{-1}, or 14.6 W m^{-2}. If we consider the same amount of precipitation falling in 3 h, we obtain 116.7 W m^{-2}, which is a significant part of the energy balance for that 3 h period, and is comparable to the amount of global short-wave radiation during cloudy and rainy days.

Ground heat flux generally plays a minor role because of the small heat conductivity of the ground and, in the case of a higher snow depth, the lack of solar radiation reaching the soil. The ground heat causes the slow ripening of the snowpack during winter and may cause slow snowmelt. The ground heat flux can be expressed as

$$Q_g = K_g \cdot \partial T / \partial z, \tag{4.8}$$

where K_g is the thermal conductivity of the soil (W m^{-1} °C^{-1}) and $\partial T/\partial z$ (°C m^{-1}) is the temperature gradient in the soil.

The internal energy of the snowpack depends on snow temperature and can be expressed as the sum of the internal energy of the three snowpack components: ice, water, and water vapor. The change in the internal energy can play a significant role for glaciers and can delay the onset of melt for snow.

Calculation of the energy balance of the snowpack is a physically based approach for modeling the snowmelt. Based on the availability of meteorological data, a wide range of approximations of the energy balance can be used. The advantage of methods based on the energy budget is their broad range of use under different climatic conditions. The energy budget approach enables snow accumulation, transformation, and melting processes to be physically represented. The main disadvantage of the energy budget method is the difficulty in obtaining the input data necessary for the parameterization, calibration, and validation of the model. It is thus difficult to use this approach

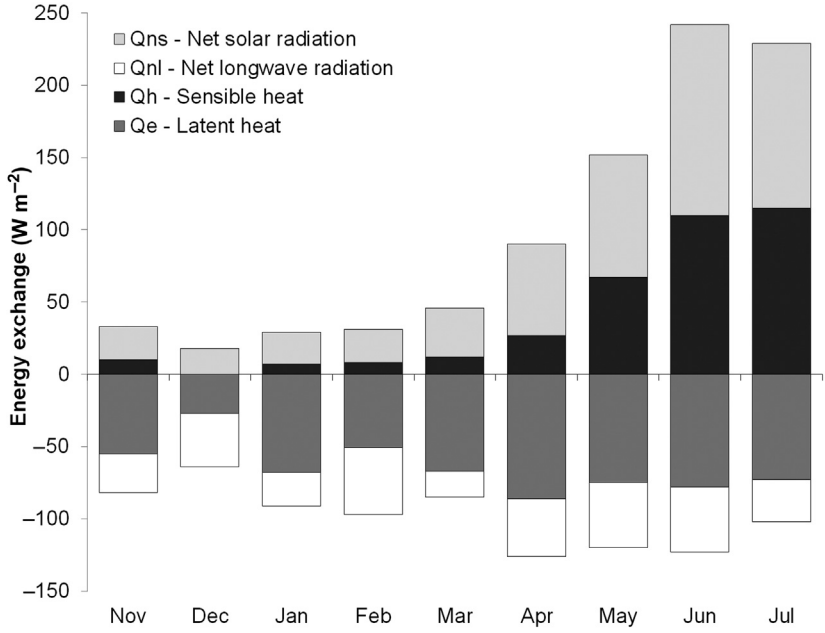

FIGURE 4.7 Seasonal variation in major snowpack energy exchange components at a Sierra Nevada alpine ridge site in 1986. *Data from Marks and Dozier, 1992.*

for calculating snow accumulation and snowmelt for ungauged catchments. Figure 4.7 shows an example of the seasonal variation in the major snowpack energy exchange components.

Energy fluxes can be converted into an amount of melted snow, as described in DeWalle and Rango (2008), where

$$M = Q_{\mathrm{m}} / \left(\rho_{\mathrm{w}} \cdot L_{\mathrm{f}} \cdot B\right), \tag{4.9}$$

where M (m d^{-1}) is the amount of melt water, Q_{m} (kJ m^{-2} d^{-1}) is the positive daily output from the energy budget, ρ_{w} is the water density ($\sim$1,000 kg m^{-3}), L_{f} is the latent heat of fusion (334 kJ kg^{-1}), and B (−) is the thermal quality of snow, which is defined as the energy necessary to melt a certain mass of snow relative to the energy necessary to melt the same mass of ice at 0 °C.

4.2.5.2 Degree-Day Method

The calculation of the individual items of the snowpack energy balance is complex and needs a lot of data that are commonly not available. To overcome the lack of data, the so-called index methods are characteristically used. These methods calculate the snowmelt using some accessible and easily measurable variable that is generally related to the energy balance. The air temperature is commonly used because of its high correlation with snow and glacier melt, and availability (Braithwaite and Olesen, 1989). Other studies have also shown the

importance of long-wave radiation and sensible heat flux on the energy budget. Both heat fluxes generally provide 75 percent of the entire energy balance, and the air temperature plays a key role in their calculation (Hock, 2003; Ohmura, 2001; Pohl et al., 2006). Approaches incorporating air temperature are referred to as temperature-index methods.

In the temperature-index method, the S_{WE} decreases according to the melt, M (mm d^{-1}) and is calculated as

$$M = m_f(T - T_T), \tag{4.10}$$

where m_f (mm $°C^{-1}$ d^{-1}) is the melt or degree-day factor, T_T is the threshold temperature for snowmelt to start, and T is the mean air temperature (both in C). The values for T_T typically vary from 0 to 2 °C. The degree-day factor generally has values between 1 and 7 mm $°C^{-1}$ d^{-1}, with lower values for forested areas (Seibert, 1999). The temperature index method has been developed for a daily time step, but has also been used for shorter or longer time intervals.

The initial storage of melt water within the snowpack can be conceptualized by a liquid water storage, which has to exceed a certain fraction of the S_{WE} before drainage from the snowpack occurs (Lindström et al., 1997). If temperatures decrease, this liquid water might refreeze, which can be simulated by an equation similar to Eqn (4.10), but with a refreezing coefficient C_{FR} (Eqn (4.11)). This coefficient typically has a value of 0.05. This means that the refreezing is 20 times less efficient than the melt, which reflects the difference that the melt occurs at the snow surface, whereas the refreezing occurs when the liquid water is distributed over the snowpack and mainly insulated against the cold.

$$R = C_{FR} \cdot m_f \cdot (T_T - T). \tag{4.11}$$

The temperature index method dates back to work by Finsterwalder and Schunk (1887) in a glaciological study in the Alps and is probably still the most widely used snowmelt method among hydrologists. Hock (2003) summarizes the advantages of the temperature index method as (1) the availability of air temperature data; (2) the relatively simple spatial distribution of the air temperature and its predictability; (3) the simplicity of the computational procedure; and (4) satisfactory results of the model despite its simplicity. Although there are clear advantages of this method, Beven (2001) formulated shortcomings of this method as (1) the accuracy of the method decreases with the increasing temporal resolution; (2) the intensity of the snowmelt has a large spatial variability depending on topographic conditions, mainly slope, aspect and land cover. This variability is very difficult to express using temperature index methods.

The shortcomings of the models based on the temperature-index method with a daily time step are apparent, mainly in cases where air temperature fluctuations are around the melting point. The mean daily air temperature indicates no snowmelt; however, the positive air temperature that occurs during the

day could cause snowmelt (Hock, 2003). In mountain areas, it is necessary to consider the change in air temperature depending on the elevation; therefore, the basin is generally divided into several elevation zones (Essery, 2003).

Several enhanced and spatially distributed temperature-index models have been developed (e.g., Hock, 1999; Pellicciotti et al., 2005) that address some of the shortcomings of the classical degree–day model. In these approaches, the degree-day factor varies as a function of potential solar radiation, and the formulation is closer to the principles of the energy balance.

The melt factor m_f is the key parameter in Eqn (4.10) and is influenced by several factors (Table 4.3). Martinec (1975) derived an empirical relation between the melt factor and the snow density as

$$m_f = 11\frac{\rho_s}{\rho_w}, \tag{4.12}$$

where m_f is the melt factor (mm $^\circ C^{-1}$ d^{-1}), ρ_s is the snow density, and ρ_w is the water density (both (kg m^{-3})). This equation reflects the tendency for the melt factor to increase in the spring, together with an increase in snow density due to the ripening process. Kuusisto (1980) derived an empirical relation between the melt factor and the snow density separately for forest and open areas:

$$\text{forest: } m_f = 0.0104\rho_s - 0.70, \tag{4.13}$$

$$\text{open areas: } m_f = 0.0196\rho_s - 2.39. \tag{4.14}$$

Forests cause a decrease in the amount of direct solar radiation that reaches the surface and therefore the snowmelt in periods without precipitation. Different melt factors were derived by Federer et al. (1972) for the northwest of the USA. They experimentally derived the melt factor 4.5–7.5 mm $^\circ C^{-1}$ d^{-1} for open areas, 2.7–4.5 mm $^\circ C^{-1}$ d^{-1} for deciduous forests, and 1.4–2.7 mm $^\circ C^{-1}$ d^{-1} for coniferous forests (approximate ratio 3:2:1). Kuusisto (1980) expressed variations in the melt factor dependent on the relative canopy cover of coniferous forests, C_{canopy} (–) with typical values of 0.1–0.7, as

$$m_f = 2.92 - 1.64C_{canopy}. \tag{4.15}$$

4.3 GLACIERS AND GLACIAL MASS BALANCE

4.3.1 Glacier Mass Balance

The glacier mass balance provides information about the amount of water stored or released by a glacier within a given time period (Cogley et al., 2011). The glacier mass budget is characteristically evaluated over one hydrological year (October 1–September 30) and is reported as water equivalent per unit area per

TABLE 4.3 Factors Influencing Melt Factor

Factor	Cause	Influence on Melt Factor
Seasonal influence	Decrease of cold content and albedo, increase in short-wave radiation and snow density	Melt factor increases
Open area versus forest	Shading and wind protection	Lower melt factor and its spatial variability in the forest
Topography (slope, aspect)	Variability of short-wave radiation and wind exposure	Higher melt factor on south-facing slopes
Snow-cover area	Spatial snowmelt variability	Melt factor decreases in the basin with larger SCA
Snowpack pollution	Dust and other pollution cause lower albedo	Higher melt factor
Precipitation	Rainfall supplies sensible heat, clouds decrease solar radiation	Generally lower melt factor on rainy days due to lower radiation. But precipitation itself causes higher melt factor.
Snow versus ice	Glacial ice has lower albedo than snow	Higher melt factor in glaciated basins
Meteorological conditions for certain air temperature	Higher snowmelt with higher wind speed, higher radiation, or higher moisture for the same temperature	Higher melt factor

Based on DeWalle and Rango, 2008.

year (m a^{-1}). Mass balance b (m a^{-1}) at one point on the glacier surface is defined as the sum of accumulation c (m a^{-1}) and ablation a (m a^{-1}) as

$$b = c + a. \tag{4.16}$$

By integrating b over the glacier surface S (Cogley et al., 2011), the glacierwide, surface mass balance B_{sfc} corresponding to the mean thickness of the water equivalent added or removed can be calculated as

$$B_{sfc} = \frac{1}{S}\int_S b\mathrm{d}S. \tag{4.17}$$

Basal ice melt and mass loss due to frontal ablation (calving, ice break-off) add to the total mass balance ΔM, but these components are comparatively small or almost negligible for most glaciers in mid- and low-latitude mountain ranges.

Mass balances can be determined using a variety of methods ranging from direct measurements on the glacier surface to techniques using remote sensing. The measurement of glacial mass changes at annual to seasonal time scales is mostly based on the glaciological method applying spatial interpolation and extrapolation of melt and accumulation measurements at a number of ablation stakes and snow pits (Kaser et al., 2003; Østrem and Stanley, 1969; Zemp et al., 2013). At time scales of a few years to several decades, the comparison of repeated information on glacier surface elevation provides accurate data on long-term volume changes of large and inaccessible glaciers (e.g., Bauder et al., 2007; Bolch et al., 2013; Paul and Haeberli, 2008). Recently, the application of satellite-based changes in the Earth's gravity field has become increasingly popular for evaluating glacier mass changes for entire mountain ranges (e.g., Gardner et al., 2013).

Most mid- and high-latitude mountain glaciers exhibit clearly separated accumulation and ablation periods (Figure 4.8(a)). Glacier storage changes are positive during the winter season with precipitation mainly falling as snow, and limited or absent melt. The ablation season is commonly concentrated over a few months with the highest air temperatures and strong solar radiation (Figure 4.8(c)). Glaciers thus store most of the winter precipitation, which is often strongly enhanced due to orographic uplift, and release it during a few summer months (Jansson et al., 2003; Stenborg, 1970). This behavior has a significant effect on the hydrological regime of glacierized drainage basins that are dominated by the components of snow and ice melt (Figure 4.8(e)).

4.3.2 The Glacial Drainage System

Glaciers are an important storage element in the hydrological cycle and are characterized by their water retention potential at different temporal and

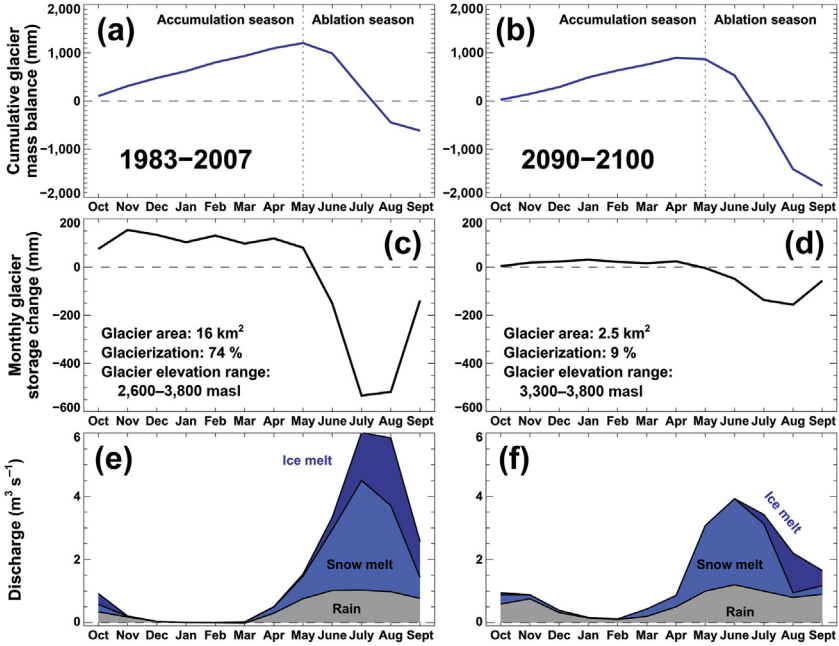

FIGURE 4.8 Glacier mass balance B_{sfc}, monthly glacier storage change and runoff components in the catchment of Findelengletscher, Switzerland, for the periods 1983−2007 and 2090−2100 based on glaciohydrological modeling *(Huss et al., 2014)*. (a,b) Cumulative glacier surface mass balance indicating limited mass losses in 1983−2007 and a strongly negative mass balance in 2090−2100. (c,d) Monthly glacier storage change relative to the water balance of the entire catchment. (e,f) Simulated components of catchment discharge (bare-ice melt, snowmelt, and rain minus evapotranspiration).

spatial scales (Jansson et al., 2003). Whereas water retention in the ice volume refers to periods of decades to centuries, englacial and subglacial water storage is highly important at shorter time scales of a few hours to days. Melt water derived from bare-ice surfaces is generally collected in supraglacial streams and is transported relatively rapidly to a moulin connecting surface water flow with the glacier bed (Figure 4.9). Melt generated in the accumulation area, however, infiltrates into porous firn and snow where it might be stored for days to months until it runs off, or where it refreezes again.

The characteristics and the development of the englacial and subglacial drainage systems determine water flow through the ice (see Fountain and Walder, 1998; for a review), as well as the hydraulic head within the glacier. Englacial water pressure exhibits a strong connection with surface ice flow over its close link to basal sliding (e.g., Iken and Bindschadler, 1986). Subglacial water flow occurs either in a rather inefficient, distributed, and interlinked system of small cavities or in individual channels at the ice−bedrock interface that promote an efficient drainage (e.g., Flowers, 2002; Röthlisberger

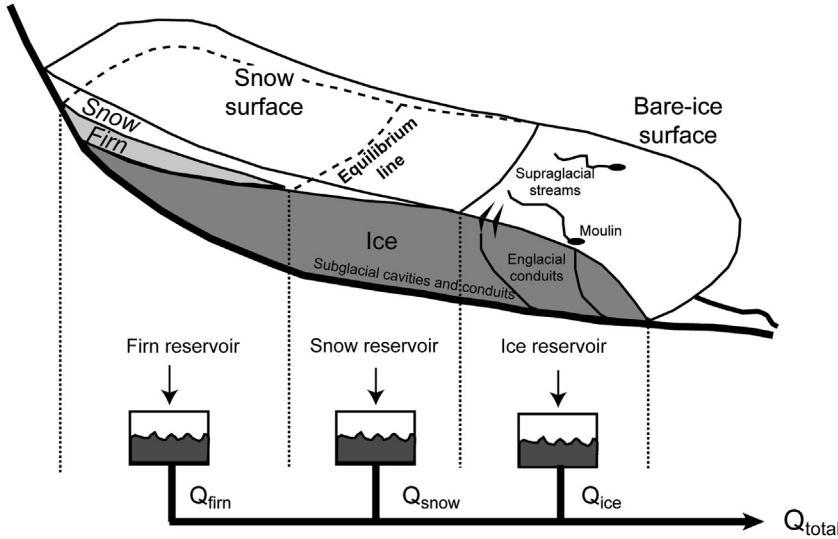

FIGURE 4.9 Schematic representation of the glacial drainage system and the approach to modeling it using linear reservoirs. *Redrawn after Hock and Jansson, 2005.*

and Lang, 1987, Figure 4.9). The subglacial drainage system develops throughout the melting season with sustained high melt water input and water pressures. Consequently, the water retention capacity of a glacier decreases with time (Hewitt et al., 2012; Hock and Hooke, 1993) and the diurnal amplitudes of runoff increase over the summer (Figure 4.10). Quantitative knowledge about the properties of the glacial drainage system and its state of evolution can be gained, for example, by dye tracing experiments (see, e.g., Finger et al., 2013; Werder and Funk, 2009).

4.3.3 Modeling Glacier Discharge

Over the last few decades, many different approaches to simulate glacier discharge have been developed. They focus on the spatiotemporal evolution of the englacial and subglacial drainage systems, the water retention capacity of glaciers, as well as on the long-term hydrological impacts of glaciers and their changes (Hock and Jansson, 2005; Hock, 2005). In the following, a brief overview of some modeling approaches is provided.

The physically based modeling of the subglacial drainage system has been attempted by a number of studies (e.g., Flowers, 2002; Hewitt et al., 2012; Schoof, 2010). By describing the processes of water cavity growth and drainage channel enlargement as functions of time-variable water pressure, water supply, the thermodynamic conditions and the ice flow, the development of the drainage system in time and space can be simulated, and the properties of subglacial water flow be inferred. Many hydrological studies however apply

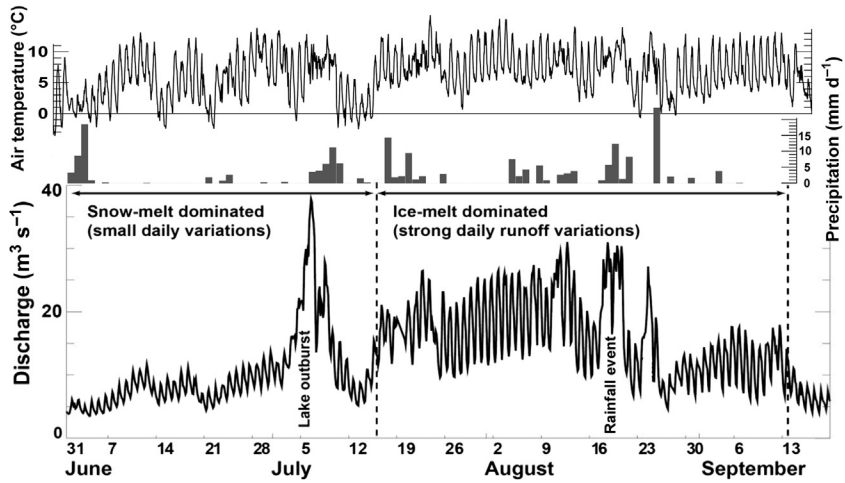

FIGURE 4.10 Runoff from the catchment of Gornergletscher (66% glacierized), Switzerland, between June and September 2004. Temperature and precipitation series of a station close to the glacier are shown for comparison while the runoff peak in July is driven by the outburst of the glacier-dammed lake, two runoff peaks in August can be attributed to rainfall events.

simpler, empirical approaches that estimate water retention and glacial runoff using linear reservoir models (Hock and Jansson, 2005). In this widely applied approach, discharge Q for each time step t is obtained from a linear relation with the volume V of hypothetical reservoirs for melt water originating from snow, firn, and bare-ice surfaces (Hock and Noetzli, 1997, Figure 4.9) as

$$Q(t) = kV(t). \tag{4.18}$$

The retention constant k is characterized by the water retention capacity of the respective reservoir and is determined by calibrating the model with field data (see, e.g., Hock, 1999).

The modeling of glacier hydrology necessarily involves the calculation of snow and ice melt as a function of the surface energy balance. Numerical methods for simulating glacier melt are similar to those for snowmelt but need to further take into account the significant albedo difference between snow and ice. Simulating runoff from glaciers over time scales of years to decades requires the description of all components of the high-alpine water balance, the snow and ice melting processes, the routing of runoff through the glacial and periglacial system. Semiempirical to process-based models have been proposed and applied with different spatial discretizations (see, e.g., Farinotti et al., 2012; Horton et al., 2006; Schaefli et al., 2007). Glaciohydrological studies over periods with strong glacier changes furthermore need to take into account the evolution of glacier area and ice thickness by physical ice-flow modeling or simplified approaches (e.g., Huss et al., 2010; Immerzeel et al., 2012).

4.4 HYDROLOGY OF SNOW- AND ICE-COVERED CATCHMENTS

4.4.1 Influence of Snow on Discharge

The most obvious feature of runoff in snow-dominated catchments is the large seasonality. Commonly, there is a more-or-less pronounced, spring flood, during which a large fraction of the annual runoff occurs during a few weeks. In highly glacierized catchments, the seasonality is even more pronounced with the runoff basically following the available energy for melt. The runoff regime of catchments without snow influence characteristically shows the opposite pattern, that is, low runoff during summer due to energy being available for evaporation. In mountainous areas, the importance of snow, and therefore also the seasonal differences, increases with elevation and the annual maximum streamflow is observed later for higher elevations (Figure 4.11(a)). In lowland catchments, a similar pattern can be observed when going from lower to higher latitudes (Figure 4.11(b)). For larger river catchments, this means that the runoff from snow and glacial melt in upstream mountainous headwater catchments can play a more important role in relative terms during summer months than on the annual average (Viviroli and Weingartner, 2004). This can be illustrated by discharge along the River Rhine (Figure 4.12): the runoff regime of the upper part is clearly dominated by snow and glacial melt, and the high summer runoff from this part of the catchment balances the low summer runoff contributions downstream.

During late summer, glacial melt contributes far more than one might expect from the proportion of the area covered by glaciers. For the month of August, for instance, glacier storage change contributes on average about 7 percent of the streamflow in River Rhine at the Andernach station, despite glaciers covering only 0.23 percent of the catchment area (Huss, 2011). The relative contribution can vary significantly and can reach >20 percent for warm summers, when both evaporation in the lower parts of the catchment is high and glacial melt is above the long-term average.

Another feature of runoff from snow-covered catchments, which is even more evident for glacierized catchments, as discussed below, is the observation of clear diurnal variations in runoff with maximum values typically in the late afternoon (Figures 4.10 and 4.13).

Despite this seasonal variation with the highest runoff in spring (on average), in smaller catchments, peak flows are generally caused by rainfall, rather than by snowmelt, because the latter is a comparatively slow process (Figures 4.13 and 4.14). Only in larger catchments do the highest flow peaks originate from snowmelt, because melting simultaneously occurs over large areas.

Rain-on-snow events are of special importance for flooding (Eiriksson et al., 2013; Floyd and Weiler, 2008; Juras et al., 2013). A common

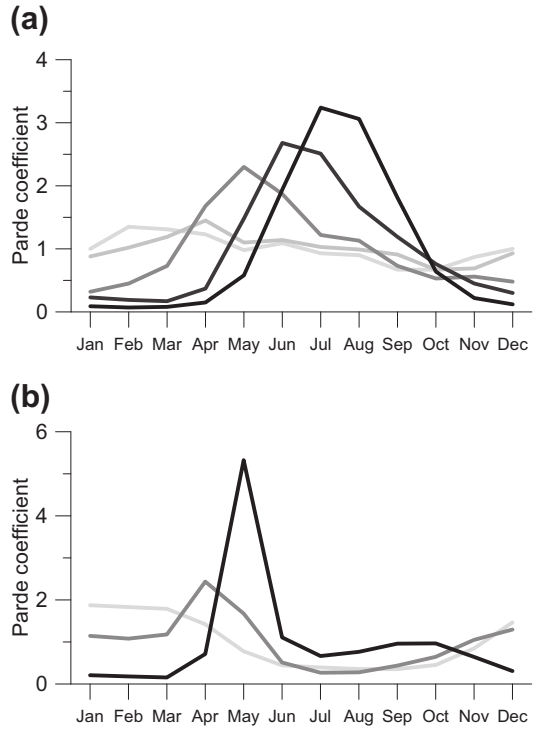

FIGURE 4.11 Seasonal runoff variation for catchments with varying snow dominance. The Pardé coefficient is the long-term monthly mean runoff divided by the annual mean. The runoff regime varies with elevation (see (a)), five catchments in Switzerland from low (light gray) to high (black) elevations: River Töss (mean elevation 650 m asl), River Goldach (830 m), River Sense (1068 m), River Minster (1351 m), River Dischmabach (2372 m), and River Rhone at Gletsch (2719 m). *(Data from Weingartner and Aschwanden, 1992)* and latitude (see (b)), three lowland catchments in Sweden from the South to the North: River Sege (light gray), River Fyris (dark gray), and River Vuoddasbäcken (black). *Data from SMHI, 1968–2012.*

misunderstanding is that the rain provides large amounts of energy to melt the snow. Energy balance calculations (see above) show that the energy added to the snowpack through rain water is small in comparison to the other energy fluxes on a daily or longer time scale. However, if rain falls on an already melting snowpack, the rainfall cannot be stored within the snowpack and it quickly percolates downward. The actual snowmelt during rain-on-snow events might be small (Mazurkiewicz et al., 2008), but an on-going snowmelt can provide wet antecedent conditions, which can lead to high flow peaks.

The above-mentioned facts cause the quick response of the catchment to the liquid precipitation (Figure 4.14). The rain-on-snow floods are characterized by a steep rising limb of the hydrograph and high flood peaks in comparison to spring floods caused by snowmelt without additional liquid

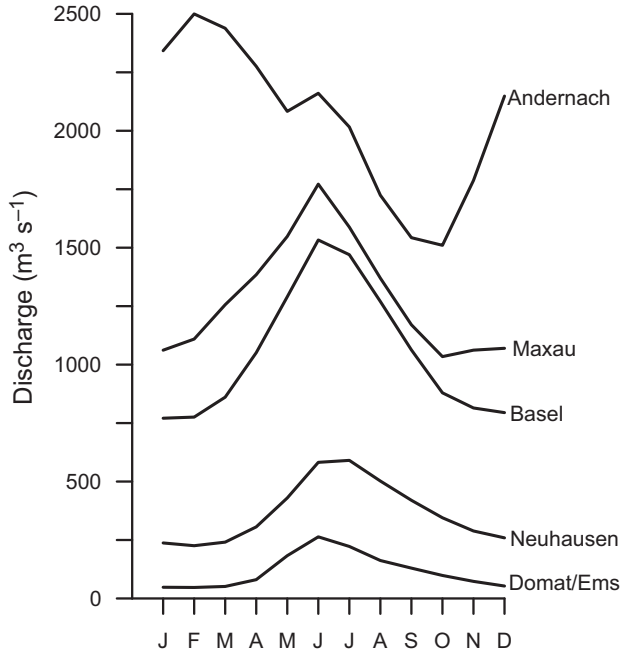

FIGURE 4.12 Seasonal runoff variation for different locations along River Rhine. *Data from Global Runoff Data Center, GRDC.*

precipitation. The total flood volume depends on the volume of liquid precipitation and melting snow. However, catastrophic flood events are most commonly caused by a combination of several unfavorable circumstances; a relatively high S_{WE} at both higher and lower elevations, air temperatures significantly above the melting point at all elevations, high liquid precipitation, windy conditions causing turbulent heat exchange, ripe snowpack (isothermal conditions), and, before the rain-on-snow event, antecedent soil moisture, frozen soils, and existing river ice.

One of the biggest rain-on-snow events and resulting floods in Central Europe on a large scale occurred in the Danube River basin during the spring of 2006. The flood mainly affected the area of the upper Danube River basin and some northern tributaries such as the Morava River, Váh River, and Tisza River. The main reasons for the flood were the unusually high quantities of snow at medium elevations, together with high air temperature and liquid precipitation. Although the liquid precipitation was important but still not extreme on a large scale (it ranged from 50 mm to around 100 mm depending on the subbasin location), the high snow storage caused extreme flood peaks with return periods up to 100 years for some subbasins, such as the Morava River and Danube River at Budapest (Wachter, 2007).

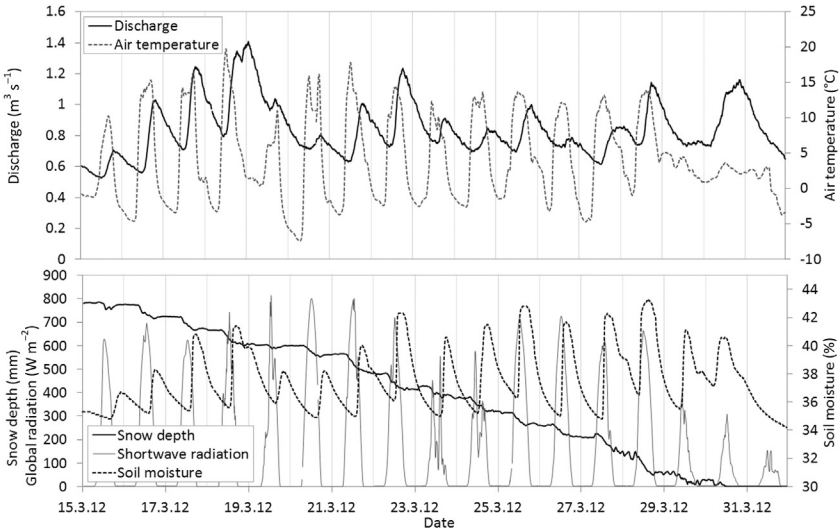

FIGURE 4.13 Snowmelt caused by high air temperature during sunny weather in the Bystřice River basin, Krušné Mts, Czech Republic. Diurnal variation of the air temperature, snow depth, soil moisture, and discharge is typical for these kinds of situations. The soil was not frozen during this period. Typical diurnal variations of the snow depth are caused by freezing conditions during night time, which temporarily stops the snowmelt. *Data from the Charles University in Prague, Faculty of Science.*

The occurrence of rain-on-snow events will probably change in the future due to the increase in air temperature and precipitation during winter. Surfleet and Tullos (2013) assessed historical and predicted runoff data for the Santiam River basin in Oregon and concluded that the peak flows associated with rain-on-snow events will decrease at lower elevations, whereas there will be a significant rise in the frequency of peak daily flows <5−10 year return period at medium to high altitudes. However, the overall frequency of rain-on-snow events was expected to decrease in the studied basin due to generally smaller amounts of snow.

4.4.2 Influence of Glaciers on Discharge

Glaciers are important elements of the hydrological cycle in alpine environments and are known to strongly influence the runoff regime of glacierized drainage basins at local to regional and larger scales, even with only a minor degree of glacier coverage (Hock, 2005; Kaser et al., 2010). The significant influence of glaciers on the hydrological regime of mountainous catchments has been well documented by a number of studies (e.g., Barnett et al., 2005; Fountain and Tangborn, 1985; Kuhn and Batlogg, 1998; Meier and Tangborn, 1961). Hock (2005) identified five specific characteristics of glacierized basins: (1) During years with glacier mass gain, specific runoff from the

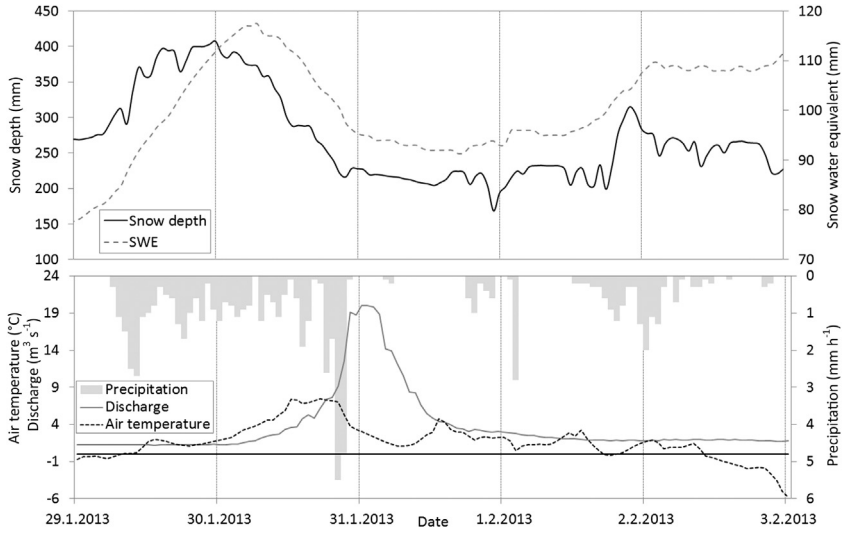

FIGURE 4.14 Rain-on-snow event from January 29, 2013, to February 3, 2013, at the Modrava climate station, Šumava Mountains, Czech Republic. The different timing of peaks for the displayed variables (snow depth, S_{WE}, air temperature, discharge) can be shown to indicate the "sponge" effect of the snowpack with metamorphic changes of ice crystals and possible accumulation of liquid water in the snowpack (a decrease of snow depth with increasing S_{WE}). *Data from the Charles University in Prague, Faculty of Science.*

catchment is reduced while in years with mass loss, additional water from long-term glacial storage contributes to discharge; (2) The runoff regime in basins with a glacierization of more than a few percent shows strong seasonal variations with small discharge over 6–8 months and peak runoff during the melting season; (3) Runoff is characterized by distinct diurnal variations with large amplitudes (Figure 4.10); (4) Basins with an intermediate glacierization exhibit reduced interannual runoff fluctuations as melt and precipitation compensate for each other (Farinotti et al., 2012; Lang, 1986); (5) Glacier runoff is positively correlated with air temperature, whereas it is negatively correlated with precipitation.

4.4.2.1 Quantifying Glacier Contribution to Runoff

Many recent studies have addressed the contribution of past, present, and future glacier melt to runoff (e.g., Huss, 2011; Immerzeel et al., 2010; Kaser et al., 2010; Koboltschnig and Schöner, 2011; Weber et al., 2010). The percentage of glacial water in streamflow is considered a good proxy for future runoff changes related to the potential disintegration of glaciers with ongoing atmospheric warming. As summarized by Radić and Hock (2014), considerable disagreement occurs in the literature about the definition of glacier contribution to runoff leading to major difficulties in comparing published estimates.

Among the six different concepts for quantifying glacier contribution detected by Radić and Hock (2014), two major groups can be separated: Some studies consider only melt water originating from the ablation area (i.e., bare-ice melt) as glacier runoff and explicitly exclude snowmelt over the glacier (e.g., Jost et al., 2012; Koboltschnig and Schöner, 2011; Racoviteanu et al., 2013; Stahl et al., 2008; Weber et al., 2010). Other papers define glacier contribution based on a water balance approach, and thus take into account all water derived from glacierized surfaces (Huss, 2011; Kaser et al., 2010; Lambrecht and Mayer, 2009; Neal et al., 2010). Evaluations of glacier contribution to runoff thus need to detail the applied approach in order to provide useful values for water resource management.

A straightforward and independent approach to determine the importance of snow and ice melt water in stream-flow runoff is the measurement of stable chemical isotopes that allow the direct quantification of the fractional contribution of the different runoff components in the analyzed sample (e.g., Collins, 1977; Finger et al., 2013; Racoviteanu et al., 2013; Taylor et al., 2001). This method is purely observational and does not require hydrological modeling or water-balance calculations for evaluating the melt water contribution. An immediate comparison to the above approaches is, however, difficult as chemical analysis only refers to particle concentrations, whereas daily to seasonal runoff variations also propagate by differences in the hydraulic head, for example, through lakes. A reliable determination of glacier contribution by chemical analysis is thus only possible in the proglacial stream, but not in large-scale catchments.

4.4.2.2 Glacier Runoff and Climate Change

Strong changes in the storage and runoff characteristic of glacierized drainage basins are expected in response to climate change over the twenty-first century (Barnett et al., 2005; Braun et al., 2000; Hock et al., 2005; Huss et al., 2008; Stahl et al., 2008). Due to glacier recession, a significant decrease in glacier storage capacity is probable—glaciers store smaller amounts of water in winter and thus release less during the melting season (Figure 4.8(d)). This reduction in the natural and beneficial capability of glaciers to smooth out runoff variability by their anticyclic behavior will be crucial in terms of water resource management (e.g., Chen and Ohmura, 1990; Schaefli et al., 2007), as well as regarding the effects of extreme years such as the European heat wave of 2003 (Zappa and Kan, 2007). Far-reaching impacts due to glacier retreat in many of the Earth's mountain ranges are thus expected to be most severe in regions with summer-dry conditions (Hagg and Braun, 2005; Immerzeel et al., 2010; Juen et al., 2007; Sorg et al., 2012). The example of Findelengletscher, Switzerland, shows that drainage basin runoff during the summer months might decrease by $\geq$50 percent due to a lack of snow and ice melt compared to the present situation (Figure 4.8).

The recent decline of glacier ice volume observed in all regions around the globe (Gardner et al., 2013) is a major concern regarding sea-level rise (see also the Chapter by Allison et al. (2014)). Until the end of the twenty-first century, melting glaciers are expected to raise global sea level by 0.1−0.2 m (Marzeion et al., 2012; Radić et al., 2014). From a hydrological perspective, it is, however, important to mention that for several reasons not all glacial melt water will immediately contribute to sea-level rise (Haeberli and Linsbauer, 2013): (1) In polar regions, glacier ice is partly grounded below sea level and is thus not a net contribution when removed. This factor accounts for a 5−10 percent reduction in sea-level rise estimates from glaciers at a global scale. (2) In a deglaciating landscape the formation of new proglacial lakes can be observed (Haeberli et al., 2012). These lake basins store some of the glacial melt water, but might also represent a serious hazard potential (Clague and O'Connor, 2014; Haeberli and Whiteman, 2014). (3) Some glacierized regions (mostly in High Mountain Asia) drain into endorheic basins that have no direct connection to the ocean. Furthermore, glacial melt water might also contribute to groundwater recharge. Overall, these factors lead to a small but systematic decrease in the sea-level rise contribution from melting glacier ice and thus need to be accounted for.

4.4.3 River Ice

River ice (Figure 4.15) is an important feature of many rivers, which can contribute to extreme events. The cooling of water during fall and winter differs for flowing river water compared to that for lakes. While in lakes after an initial cooling to about 4 °C, a thermal stratification develops with only the upper water layer cooling down further, generally the entire water column cools down at the same rate in rivers due to the mixing of the flowing water. The cooling is mainly caused by the negative, long-wave radiation budget, the convective heat transfer to the atmosphere, and the cooling effect of evaporation. Precipitation can have some cooling effect, especially in the case of

FIGURE 4.15 Water, snow, and ice in the Roseg Valley, Pontresina, Switzerland.

snow when energy is consumed for melting. Groundwater is characteristically the main contribution to river flow and can be a significant source of energy due to the higher temperatures. When river water cools down to 0 °C, various types of ice can form (Prowse, 2005). These include border ice along the river banks and frazil ice. The latter is made up of loose ice crystals that start forming when the water is supercooled (<-0.05 °C), and both grow and aggregate into larger ice pieces. With continued cooling eventually a complete ice cover can develop. This ice cover can breakup depending on factors such as ice thickness and strength, river geometry, flow velocity, and water levels. In cold climates, ice breakup occurs usually as one major spring event. The importance of this type of event in cold climates is also indicated by many historical records, which have been used as climatological indicators, especially for times before measurements started (Kajander, 1993; Magnuson et al., 2000; Rannie, 1983). In more temperate climates, there might be several freeze−breakup cycles during one winter season. During ice breakup, high water levels can be caused by ice dams, and severe flooding might be due to failure of such ice dams (Prowse, 2005). Although river ice can cause high flows, the more surprising observation is also that runoff in winter and spring can be affected by temporary water storage within rivers driven by hydraulic friction in situations with river ice (Prowse and Carter, 2002). Winter runoff thus decreases, and spring runoff is enhanced.

4.4.4 Permafrost and Seasonally Frozen Soils

The freezing of soil, both permanently and seasonally, can have significant impacts on runoff generation processes (Hayashi, 2013). Soil freezing starts when the temperatures at the soil surface decrease below zero degrees, which causes a temperature gradient toward the surface from the so-called freezing front. The soil energy balance is highly dependent on the presence of a snow cover. Due to the low thermal conductivity of snow, snow has an insulating effect, and a snow cover of 20−30 cm is enough to inhibit further freezing from above (Hirota et al., 2006), whereas freezing from below in permafrost regions occurs independently of snow cover. In ice-rich frozen soils, conductive heat transfer is dominant because the ice prevents advective transfer by liquid water or vapor, which would otherwise be more important. The largest effect of soil frost on runoff generation is the changed infiltration capacity. Detailed modeling of soil frost and its effects on hydraulic conductivity is challenging, and approaches such as using two flow domains (slow and quick flow) have to be used to better predict water fluxes in frozen soils (Stähli et al., 1996, 1999). A general observation, however, is that the soil water content at the time of freezing largely influences the resulting infiltration capacity. In the case of wet soils at the beginning of freezing, the frozen soil can form an almost impermeable layer. This can generate a complex interaction between climate, snow, and runoff. For instance, in boreal catchments, higher runoff peaks might be observed after snow-poor winters, compared to

after snow-rich winters, which might seem counterintuitive at first. The explanation is that during winters with less snow, there is less insulation and deeper frozen soil will develop, which in turn would lead to restricted infiltration and thus higher runoff peaks. Because snow depth and soil frost are generally inversely correlated, the presence of soil frost might seldom lead to extreme floods (Lindström et al., 2002). However, the interplay between snow accumulation and soil frost is complex, and the conditions during early winter are most important (Bayard et al., 2005; Stähli et al., 2001). In many areas, especially within forests, soil frost does not generally fully stop infiltration, but rates can be significantly reduced. In wetlands, on the other hand, soil frost can generate an impermeable layer and cause overland flow (Laudon et al., 2007). On a larger scale, the effect of other factors commonly masks a clear relationship between snow accumulation, soil frost, and runoff (Shanley and Chalmers, 1999).

Permafrost can have even larger effects on hydrological processes. Permafrost is subsurface ground material (soil, sediment, bedrock, etc.) that has a temperature below 0 °C for consecutive years and exists in about 20–25 percent of the Earth's land surface (Dankers, 2008). In areas with permafrost, the upper parts of the ground generally thaw and refreeze seasonally. This part of the ground is termed the "active layer" and begins to form during spring snowmelt and reaches its greatest depth in late summer/early fall. This means that the ground portion that is available for infiltration and liquid water storage increases during the summer and then again decreases during winter. Ice-rich permafrost can decrease the hydraulic conductivity of the ground dramatically, so that an almost impermeable layer can be formed. In this case, groundwater (or saturated conditions) can be found both seasonally in the active layer above the perennially frozen part of the ground and below this zone. With the impermeable layer, permafrost can result in increased soil moisture in the active layer, and might even result in perched lakes. Where water infiltrates into the deeper groundwater in areas with higher elevations, confined aquifers with artesian wells can be formed in neighboring areas of lower elevation (Hinzman et al., 2005). When permafrost thaws due to climate change, the active layer becomes deeper, and the streamflow dynamics might change. For a catchment in Northern Sweden, observed changes in streamflow dynamics quantified by recession coefficients could be linked to permafrost thawing rates (Lyon et al., 2009). Increasing temperatures also cause permafrost degradation and surface subsidence (Streletskyi, 2014). One important consequence of melting permafrost in mountainous areas is an increased risk for slope failures due to a decrease in slope stability (Deline and Gruber, 2014).

4.5 CONCLUDING REMARKS

In this chapter, we discussed various aspects of snow and ice in the water cycle. In cold climates, the freezing–thawing threshold is crucial for many processes influencing the hydrology at different scales. Due to this

temperature threshold, snow- and glacier-dominated catchments might react very sensitively to climate variations, especially for those parts of the year where temperatures today are around 0 °C. In general, it is expected that higher temperatures will shorten the snow season, and reduce glacier storage capacity, leading to changes in seasonal runoff. Although the exact impacts on the length of the snow cover period will vary, one can estimate that with a mean temperature increase of 3 °C, the snow-cover period can be easily shortened by about a month. Besides direct impacts on the hydrology, this also has indirect impacts through possible changes in the vegetation, because the extension of the part of the year without snow cover implies a prolongation of the growing season. As discussed above, with a decreased snow cover in winter, higher temperatures might paradoxically lead to an increased cooling of soils due to the missing insulation of the snow. For permafrost areas, the deeper active layer might result in increased infiltration rates and storage and thus reduced overland flow. A good understanding of the role of snow and ice in the hydrology of cold region catchments is crucial for addressing natural hazards and water management in these sensitive systems, both today and in the future. Due to the characteristically difficult conditions, field observations are still limiting our knowledge of the hydrological processes in these regions, and further studies combining field observations and modeling are needed for an improved understanding.

REFERENCES

Allison, I., Colgan, W., King, M., Paul, F., 2014. Ice sheets, glaciers and sea-level rise. In: Haeberli, W., Whiteman, C. (Eds.), Snow and Ice-Related Hazard, Risks and Disasters. Elsevier, pp. 713–747.

Anderton, S.P., White, S.M., Alvera, B., 2004. Evaluation of spatial variability in snow water equivalent for a high mountain catchment. Hydrol. Process. 18, 435–453.

Arenson, L.U., Colgan, W., Marshall, H.P., 2014. Physical, mechanical and thermal properties of snow, ice and permafrost. In: Haeberli, W., Whiteman, C. (Eds.), Snow and Ice-Related Hazard, Risks and Disasters. Elsevier, pp. 35–75.

Barnett, T.P., Adam, J.C., Lettenmaier, D.P., 2005. Potential impacts of a warming climate on water availability in snow-dominated regions. Nature 438, 303–309.

Bauder, A., Funk, M., Huss, M., 2007. Ice-volume changes of selected glaciers in the Swiss Alps since the end of the 19th century. Ann. Glaciol. 46, 145–149.

Bavera, D., Bavay, M., Jonas, T., Lehning, M., De Michele, C., 2014. A comparison between two statistical and a physically-based model in snow water equivalent mapping. Adv. Water Resour. 63, 167–178.

Bayard, D., Stähli, M., Parriaux, A., Flühler, H., 2005. The influence of seasonally frozen soil on the snowmelt runoff at two Alpine sites in southern Switzerland. J. Hydrol. 309, 66–84.

Bernhardt, M., Schulz, K., Liston, G.E., Zängl, G., 2012. The influence of lateral snow redistribution processes on snow melt and sublimation in alpine regions. J. Hydrol. 424-425, 196–206.

Beven, K.J., 2001. Rainfall-runoff Modelling: The Primer. Wiley, Chichester.
Bolch, T., Sandberg Sørensen, L., Simonsen, S.B., Mölg, N., Machguth, H., Rastner, P., Paul, F., 2013. Mass loss of Greenland's glaciers and ice caps 2003–2008 revealed from ICESat laser altimetry data. Geophys. Res. Lett. 40, 875–881.
Braithwaite, R.J., Olesen, O.B., 1989. Calculation of glacier ablation from air-temperature, west Greenland. In: Oerlemans, J. (Ed.), Glacier Fluctuations and Climatic Change, Glaciology and Quaternary Geology. Kluwer Academic Publishers, Dordrecht, pp. 219–233.
Braun, L.N., Weber, M., Schulz, M., 2000. Consequences of climate change for runoff from Alpine regions. Ann. Glaciol. 31, 19–25.
Brown, R.D., Goodison, B.E., 2005. Snow cover. In: Anderson, M.G. (Ed.), Encyclopedia of Hydrological Sciences. John Wiley and Sons, Chichester, UK, pp. 1–12.
Chen, J., Ohmura, A., 1990. Estimation of Alpine glacier water resources and their change since the 1870s. In: Hydrology in Mountainous Regions. I—Hydrological Measurements; the Water Cycle (Proceedings of Two Lausanne Symposia, August 1990). IAHS Publ, pp. 127–136. No. 193.
Clague, J.J., O'Connor, J.E., 2014. Lake outbursts. In: Haeberli, W., Whiteman, C. (Eds.), Snow and Ice Related Hazard, Risks and Disasters. Elsevier, pp. 487–519.
Cogley, J.G., Hock, R., Rasmussen, L.A., Arendt, A.A., Bauder, A., Braithwaite, R.J., Jansson, P., Kaser, G., Nicholson, L., Zemp, M., 2011. Glossary of Glacier Mass Balance and Related Terms, IHP-VII Technical Documents in Hydrology No. 86. IACS Contribution No. 2, Paris.
Collins, D.N., 1977. Hydrology of an Alpine glacier as indicated by the chemical composition of meltwater. Z. für Gletscherkd. Glazialgeol. 13, 219–238.
Dankers, R., 2008. Arctic and snow hydrology. In: Bierkens, M.F.P., Dolman, A.J., Troch, P.A. (Eds.), Climate and the Hydrological Cycle. International Association of Hydrological Sciences, pp. 137–156.
Davison, B., Pietroniro, A., 2005. Hydrology of snow covered basins. In: Anderson, M.G. (Ed.), Encyclopedia of Hydrological Sciences. John Wiley and Sons, Chichester, UK, pp. 1–19.
Deline, P., Gruber, S., et al., 2014. Ice loss and slope stability. In: Haeberli, W., Whiteman, C. (Eds.), Snow and Ice Related Hazard, Risks and Disasters. Elsevier, pp. 521–561.
DeWalle, D.R., Rango, A., 2008. Principles of Snow Hydrology. Cambridge University Press, Cambridge.
Dingman, S.L., 2008. Physical Hydrology, Second ed. Waveland Pr Inc.
Eckerstorfer, M., Christiansen, H.H., 2012. Meteorology, topography and snowpack conditions causing two extreme mid-winter slush and wet slab avalanche periods in high Arctic maritime Svalbard. Permafr. Periglac. Process. 23, 15–25.
Egli, L., Jonas, T., Grünewald, T., Schirmer, M., Burlando, P., 2012. Dynamics of snow ablation in a small Alpine catchment observed by repeated terrestrial laser scans. Hydrol. Process. 26, 1574–1585.
Egli, L., Jonas, T., Meister, R., 2009. Comparison of different automatic methods for estimating snow water equivalent. Cold Reg. Sci. Technol. 57, 107–115.
Eiriksson, D., Whitson, M., Luce, C.H., Marshall, H.P., Bradford, J., Benner, S.G., Black, T., Hetrick, H., McNamara, J.P., 2013. An evaluation of the hydrologic relevance of lateral flow in snow at hillslope and catchment scales. Hydrol. Process. 27, 640–654.
Essery, R., 2003. Aggregated and distributed modelling of snow cover for a high-latitude basin. Glob. Planet. Change 38, 115–120.
Farinotti, D., Magnusson, J., Huss, M., Bauder, A., 2010. Snow accumulation distribution inferred from time-lapse photography and simple modelling. Hydrol. Process. 24, 2087–2097.

Farinotti, D., Usselmann, S., Huss, M., Bauder, A., Funk, M., 2012. Runoff evolution in the Swiss Alps: projections for selected high-alpine catchments based on ENSEMBLES scenarios. Hydrol. Process. 26, 1909–1924.

Federer, C.A., Pierce, R.S., Hornbeck, J.W., 1972. Snow management seems unlikely in the Northeast. In: Proceedings Symposium on Watersheds in Transition. American Water Resources Association, pp. 212–219.

Fierz, C., Armstrong, R.L., Durand, Y., Etchevers, P., Greene, E., McClung, D.M., Nishimura, K., Satyawali, P.K., Sokratov, S.A., 2009. The International Classification for Seasonal Snow on the Ground. IHP-VII Technical Documents in Hydrology N°83. IACS Contribution N°1, UNESCO-IHP, Paris.

Finger, D., Hugentobler, A., Huss, M., Voinesco, A., Wernli, H., Fischer, D., Weber, E., Jeannin, P.-Y., Kauzlaric, M., Wirz, A., Vennemann, T., Hüsler, F., Schädler, B., Weingartner, R., 2013. Identification of glacial meltwater runoff in a karstic environment and its implication for present and future water availability. Hydrol. Earth Syst. Sci. 17, 3261–3277.

Finsterwalder, S., Schunk, H., 1887. Der Suldenferner. Z. des Dtsch. Österreichischen Alpenvereins 18, 72–89.

Flowers, G.E., 2002. A multicomponent coupled model of glacier hydrology 1. Theory and synthetic examples. J. Geophys. Res. 107, 2287.

Floyd, W., Weiler, M., 2008. Measuring snow accumulation and ablation dynamics during rain-on-snow events: innovative measurement techniques. Hydrol. Process. 22, 4805–4812.

Fountain, A.G., Tangborn, W.V., 1985. The effect of glaciers on streamflow variations. Water Resour. Res. 21, 579–586.

Fountain, A.G., Walder, S., 1998. Water flow through temperate glaciers. Rev. Geophys, 299–328.

Gardner, A.S., Moholdt, G., Cogley, J.G., Wouters, B., Arendt, A.A., Wahr, J., Berthier, E., Hock, R., Pfeffer, W.T., Kaser, G., Ligtenberg, S.R.M., Bolch, T., Sharp, M.J., Hagen, J.O., van den Broeke, M.R., Paul, F., 2013. A reconciled estimate of glacier contributions to sea level rise: 2003 to 2009. Science (80) 340, 852–857.

Garvelmann, J., Pohl, S., Weiler, M., 2013. From observation to the quantification of snow processes with a time-lapse camera network. Hydrol. Earth Syst. Sci. 17, 1415–1429.

Grünewald, T., Schirmer, M., Mott, R., Lehning, M., 2010. Spatial and temporal variability of snow depth and ablation rates in a small mountain catchment. Cryosphere 4, 215–225.

Haeberli, W., Linsbauer, A., 2013. Global glacier volumes and sea level—small but systematic effects of ice below the surface of the ocean and of new local lakes on land. Cryosphere 7, 817–821.

Haeberli, W., Whiteman, C., 2014. In: Haeberli, W., Whiteman, C. (Eds.), Snow and Ice-Related Hazards, Risks and Disasters - A general Framework. Elsevier, pp. 1–34.

Haeberli, W., Schleiss, A., Linsbauer, A., Künzler, M., Bütler, M., 2012. Gletscherschwund und neue Seen in den Schweizer Alpen. Wasser Energ. Luft 104, 93–102.

Hagg, W., Braun, L., 2005. The influence of glacier retreat on water yield from high mountain areas: comparison of Alps and Central Asia. In: de Jong, C., Collins, D., Ranzi, R. (Eds.), Climate and Hydrology of Mountain Areas. John Wiley & Sons, Ltd, Chichester, UK, pp. 263–275.

Hayashi, M., 2013. The cold vadose zone: hydrological and ecological significance of frozen-soil processes. Vadose Zo. J., 1–8.

Hendriks, M.R., 2010. Introduction to Physical Hydrology. Oxford University Press.

Hewitt, I.J., Schoof, C., Werder, M.A., 2012. Flotation and free surface flow in a model for subglacial drainage. Part 2. Channel flow. J. Fluid Mech. 702, 157–187.

Hinzman, L.D., Kane, D.L., Woo, M., 2005. Permafrost hydrology. In: Anderson, M.G. (Ed.), Encyclopedia of Hydrological Sciences. John Wiley and Sons, Chichester, UK, pp. 1–15.
Hirota, T., Iwata, Y., Hayashi, M., Suzuki, S., Hamasaki, T., Sameshima, R., Takayabu, I., 2006. Decreasing soil–frost depth and its relation to climate change in Tokachi, Hokkaido, Japan. J. Meteorol. Soc. Jpn. 84, 821–833.
Hock, R., 1999. A distributed temperature-index ice- and snowmelt model including potential direct solar radiation. J. Glaciol. 45, 101–111.
Hock, R., 2003. Temperature index melt modelling in mountain areas. J. Hydrol. 282, 104–115.
Hock, R., 2005. Glacier melt: a review of processes and their modelling. Prog. Phys. Geogr. 29, 362–391.
Hock, R., Hooke, R.L., 1993. Evolution of the internal drainage system in the lower part of the ablation area of Storglaciären. Sweden. Geol. Soc. Am. Bull. 105, 537–546.
Hock, R., Jansson, P., 2005. Modeling glacier hydrology. In: Anderson, M.G. (Ed.), Encyclopedia of Hydrological Sciences. John Wiley and Sons, Chichester, UK, pp. 1–9.
Hock, R., Noetzli, C., 1997. Areal melt and discharge modelling of Storglaciaren. Sweden. Ann. Glaciol. 24, 211–216.
Hock, R., Jansson, P., Braun, L., 2005. Modelling the response of mountain glacier discharge to climate warming. Glob. Chang. Mt. Reg, 243–252.
Holko, L., Škvarenina, J., Kostka, Z., Frič, M., Staroň, J., 2009. Impact of spruce forest on rainfall interception and seasonal snow cover evolution in the western Tatra mountains, Slovakia. Biologia (Bratisl) 64, 594–599.
Hood, J.L., Hayashi, M., 2010. Assessing the application of a laser rangefinder for determining snow depth in inaccessible alpine terrain. Hydrol. Earth Syst. Sci. 14, 901–910.
Horton, P., Schaefli, B., Mezghani, A., Hingray, B., Musy, A., 2006. Assessment of climate-change impacts on alpine discharge regimes with climate model uncertainty. Hydrol. Process. 20, 2091–2109.
Huss, M., 2011. Present and future contribution of glacier storage change to runoff from macro-scale drainage basins in Europe. Water Resour. Res. 47, 1–14.
Huss, M., Farinotti, D., Bauder, A., Funk, M., 2008. Modelling runoff from highly glacierized alpine drainage basins in a changing climate. Hydrol. Process. 22, 3888–3902.
Huss, M., Jouvet, G., Farinotti, D., Bauder, A., 2010. Future high-mountain hydrology: a new parameterization of glacier retreat. Hydrol. Earth Syst. Sci. 14, 815–829.
Huss, M., Zemp, M., Joerg, P.C., Salzmann, N., 2014. High uncertainty in 21st century runoff projections from glacierized basins. J. Hydrol. 510, 35–48.
Iken, A., Bindschadler, R.A., 1986. Combined measurements of subglacial water pressure and surface velocity of Findelengletscher, Switzerland: conclusions about drainage system and sliding mechanism. J. Glaciol. 32, 101–119.
Immerzeel, W.W., Shrestha, A.B., Bierkens, M.F.P., Beek, L.P.H., Konz, M., 2012. Hydrological response to climate change in a glacierized catchment in the Himalayas. Clim. Change 110, 721–736.
Immerzeel, W.W., van Beek, L.P.H., Bierkens, M.F.P., 2010. Climate change will affect the Asian water towers. Science (80) 328, 1382–1385.
Jansson, P., Hock, R., Schneider, T., 2003. The concept of glacier storage: a review. J. Hydrol. 282, 116–129.
Jeníček, M., Beitlerová, H., Hasa, M., Kučerová, D., Pevná, H., Podzimek, S., 2012. Modeling snow accumulation and snowmelt runoff—present approaches and results. Acta Univ. Carolinae, Geogr. 47, 15–24.

Jonas, T., Marty, C., Magnusson, J., 2009. Estimating the snow water equivalent from snow depth measurements in the Swiss Alps. J. Hydrol. 378, 161–167.

Jost, G., Dan Moore, R., Weiler, M., Gluns, D.R., Alila, Y., 2009. Use of distributed snow measurements to test and improve a snowmelt model for predicting the effect of forest clear-cutting. J. Hydrol. 376, 94–106.

Jost, G., Moore, R.D., Menounos, B., Wheate, R., 2012. Quantifying the contribution of glacier runoff to streamflow in the upper Columbia River Basin, Canada. Hydrol. Earth Syst. Sci. 16, 849–860.

Jost, G., Weiler, M., Gluns, D.R., Alila, Y., 2007. The influence of forest and topography on snow accumulation and melt at the watershed-scale. J. Hydrol. 347, 101–115.

Juen, I., Kaser, G., Georges, C., 2007. Modelling observed and future runoff from a glacierized tropical catchment (Cordillera Blanca, Perú). Glob. Planet. Change 59, 37–48.

Juras, R., Pavlásek, J., Děd, P., Tomášek, V., Máca, P., 2013. A portable simulator for investigating rain-on-snow events. Z. für Geomorphol. 57 (Suppl), 73–89.

Kajander, J., 1993. Methodological aspects on river cryophenology exemplified by a tricentennial break-up time series from Tornio. Geophysical 29, 73–95.

Kaser, G., Fountain, A., Jansson, P., 2003. A Manual for Monitoring the Mass Balance of Mountain Glaciers. IHP-VI Technical Documents in Hydrology, Paris.

Kaser, G., Grosshauser, M., Marzeion, B., 2010. Contribution potential of glaciers to water availability in different climate regimes. Proc. Natl. Acad. Sci. U.S.A 107, 20223–20227.

Koboltschnig, G.R., Schöner, W., 2011. The relevance of glacier melt in the water cycle of the Alps: the example of Austria. Hydrol. Earth Syst. Sci. 15, 2039–2048.

Kuhn, M., Batlogg, N., 1998. Glacier runoff in Alpine headwaters in a changing climate. In: Hydrology, Water Resources and Ecology in Headwaters (Proceedings of the HeadWater'98 Conference Held at Meran/Merano, Italy, April 1998). IAHS Publ., pp. 79–88. No. 248.

Kuusisto, E., 1980. On the values and variability of degree-day melting factor in Finland. Nord. Hydrol. 11, 235–242.

Lambrecht, A., Mayer, C., 2009. Temporal variability of the non-steady contribution from glaciers to water discharge in western Austria. J. Hydrol. 376, 353–361.

Lang, H., 1986. Forecasting meltwater runoff from snow-covered areas and from glacier basins. In: Kraijenhoff, D.A., Moll, J.R. (Eds.), River Flow Modelling and Forecasting Water Science and Technology Library, Volume 3. Springer, Netherlands, pp. 99–127.

Laudon, H., Sjöblom, V., Buffam, I., Seibert, J., Mörth, M., 2007. The role of catchment scale and landscape characteristics for runoff generation of boreal streams. J. Hydrol. 344, 198–209.

Lehning, M., Löwe, H., Ryser, M., Raderschall, N., 2008. Inhomogeneous precipitation distribution and snow transport in steep terrain. Water Resour. Res. 44, 1–19.

Lindström, G., Bishop, K., Löfvenius, M.O., 2002. Soil frost and runoff at Svartberget, northern Sweden—measurements and model analysis. Hydrol. Process. 16, 3379–3392.

Lindström, G., Johansson, B., Persson, M., Gardelin, M., Bergström, S., 1997. Development and test of the distributed HBV-96 hydrological model. J. Hydrol. 201, 272–288.

López-Moreno, J.I., Stähli, M., Lopezmoreno, J., Stahli, M., 2008. Statistical analysis of the snow cover variability in a subalpine watershed: assessing the role of topography and forest interactions. J. Hydrol. 348, 379–394.

Luce, C.H., Tarboton, D.G., Cooley, K.R., 1998. The influence of the spatial distribution of snow on basin-averaged snowmelt. Hydrol. Process. 12, 1671–1683.

Lundberg, A., Richardson-Näslund, C., Andersson, C., 2006. Snow density variations: consequences for ground-penetrating radar. Hydrol. Process. 20, 1483–1495.

Lyon, S.W., Destouni, G., Giesler, R., Humborg, C., Mörth, M., Seibert, J., Karlsson, J., Troch, P.A., 2009. Estimation of permafrost thawing rates in a sub-arctic catchment using recession flow analysis. Hydrol. Earth Syst. Sci. Discuss. 6, 63–83.

Magnuson, J.J., Robertson, D.M., Benson, B.J., Wynne, R.H., Livingstone, D.M., Arai, T., Assel, R.A., Barry, R.G., Card, V., Kuusisto, E., Granin, N.G., Prowse, T.D., Stewart, K.M., Vuglinski, V.S., 2000. Historical trends in lake and river ice cover in the northern hemisphere. Science (80) 289, 1743–1746.

Maidment, D.R., 1992. Handbook of Hydrology. McGraw-Hill Professional, New York.

Marks, D., Dozier, J., 1992. Climate and energy exchange at the snow surface in the Alpine region of the Sierra Nevada: 2. Snow cover energy balance. Water Resour. Res. 28, 3043–3054.

Martinec, J., 1975. Snowmelt–runoff model for stream flow forecasts. Nord. Hydrol. 6, 145–154.

Marzeion, B., Jarosch, A.H., Hofer, M., 2012. Past and future sea-level change from the surface mass balance of glaciers. Cryosphere 6, 1295–1322.

Mazurkiewicz, A.B., Callery, D.G., McDonnell, J.J., 2008. Assessing the controls of the snow energy balance and water available for runoff in a rain-on-snow environment. J. Hydrol. 354, 1–14.

Meier, M.F., Tangborn, W.V., 1961. Distinctive characteristics of glacier runoff. US Geol. Surv. Prof. Pap. 424-B, 14–16.

Molotch, N.P., Margulis, S.A., 2008. Estimating the distribution of snow water equivalent using remotely sensed snow cover data and a spatially distributed snowmelt model: a multi-resolution, multi-sensor comparison. Adv. Water Resour. 31, 1503–1514.

Neal, E.G., Hood, E., Smikrud, K., 2010. Contribution of glacier runoff to freshwater discharge into the Gulf of Alaska. Geophys. Res. Lett. 37, 1–5.

Ohmura, A., 2001. Physical basis for the temperature-based melt-index method. J. Appl. Meteorol. 40, 753–761.

Østrem, G., Stanley, A., 1969. Glacier Mass-balance Measurements: A Manual for Field and Office Work. Canadian Department of Energy, Mines and Resources.

Paul, F., Haeberli, W., 2008. Spatial variability of glacier elevation changes in the Swiss Alps obtained from two digital elevation models. Geophys. Res. Lett. 35, 1–5.

Peck, E.L., Bissell, V.C., Jones, E.B., Burge, D.L., 1971. Evaluation of snow water equivalent by airborne measurement of passive terrestrial gamma radiation. Water Resour. Res. 7, 1151–1159.

Pellicciotti, F., Brock, B., Strasser, U., Burlando, P., Funk, M., Corripio, J., 2005. An enhanced temperature-index glacier melt model including the shortwave radiation balance: development and testing for Haut Glacier d'Arolla, Switzerland. J. Glaciol. 51, 573–587.

Pohl, S., Marsh, P., Liston, G.E., 2006. Spatial-temporal variability in turbulent fluxes during spring snowmelt. Arct. Antarct. Alp. Res. 38, 136–146.

Prokop, A., 2008. Assessing the applicability of terrestrial laser scanning for spatial snow depth measurements. Cold Reg. Sci. Technol. 54, 155–163.

Prowse, T., Carter, T., 2002. Significance of ice-induced storage to spring runoff: a case study of the Mackenzie River. Hydrol. Process. 16, 779–788.

Prowse, T.D., 2005. River-ice hydrology. In: Anderson, M.G. (Ed.), Encyclopedia of Hydrological Sciences. John Wiley and Sons, Chichester, UK, pp. 1–21.

Racoviteanu, A.E., Armstrong, R., Williams, M.W., 2013. Evaluation of an ice ablation model to estimate the contribution of melting glacier ice to annual discharge in the Nepal Himalaya. Water Resour. Res. 49, 5117–5133.

Radić, V., Bliss, A., Beedlow, A.C., Hock, R., Miles, E., Cogley, J.G., 2014. Regional and global projections of twenty-first century glacier mass changes in response to climate scenarios from global climate models. Clim. Dyn. 42, 37–58.

Radić, V., Hock, R., 2014. Glaciers in the Earth's hydrological cycle: Assessments of glacier mass and runoff changes on global and regional scales. In The Earth's Hydrological Cycle (pp. 813–837). Springer Netherlands.

Rannie, W.F., 1983. Breakup and freezeup of the Red River at Winnipeg, Manitoba Canada in the 19th century and some climatic implications. Clim. Change 5, 283–296.

Rasmussen, R., Baker, B., Kochendorfer, J., Meyers, T., Landolt, S., Fischer, A.P., Black, J., Thériault, J.M., Kucera, P., Gochis, D., Smith, C., Nitu, R., Hall, M., Ikeda, K., Gutmann, E., 2012. How well are we measuring snow: the NOAA/FAA/NCAR Winter precipitation test bed. Bull. Am. Meteorol. Soc. 93, 811–829.

Röthlisberger, H., Lang, H., 1987. Glacial hydrology. In: Gurnell, M., Clark, M.J. (Eds.), Glacio-fluvial Sediment Transfer: An Alpine Perspective. John Wiley & Sons, Ltd, Chichester, UK, pp. 207–284.

Schaefli, B., Hingray, B., Musy, A., 2007. Climate change and hydropower production in the Swiss Alps: quantification of potential impacts and related modelling uncertainties. Hydrol. Earth Syst. Sci. 11, 1191–1205.

Schelker, J., Kuglerová, L., Eklöf, K., Bishop, K., Laudon, H., 2013. Hydrological effects of clear-cutting in a boreal forest—snowpack dynamics, snowmelt and streamflow responses. J. Hydrol. 484, 105–114.

Schoof, C., 2010. Ice-sheet acceleration driven by melt supply variability. Nature 468, 803–806.

Schweizer, J., Bartelt, P., van Herwijnen, A., 2014. Snow avalanches. In: Haeberli, W., Whiteman, C. (Eds.), Snow and Ice-Related Hazards, Risks and Disasters. Elsevier, pp. 395–436.

Seibert, J., 1999. Regionalisation of parameters for a conceptual rainfall-runoff model. Agric. For. Meteorol. 98-99, 279–293.

Seidel, K., Martinec, J., 2010. Remote Sensing in Snow Hydrology—Runoff Modelling, Effect of Climate Change. Springer Verlag.

Sevruk, B., Ondrás, M., Chvíla, B., 2009. The WMO precipitation measurement intercomparisons. Atmos. Res. 92, 376–380.

Shanley, J.B., Chalmers, A., 1999. The effect of frozen soil on snowmelt runoff at Sleepers River, Vermont. Hydrol. Process. 13, 1843–1857.

Singh, P., Singh, V.P., 2001. Snow and Glacier Hydrology. Kluwer Academic Publishers, London.

Sold, L., Huss, M., Hoelzle, M., Andereggen, H., Joerg, P.C., Zemp, M., 2013. Methodological approaches to infer end-of-winter snow distribution on alpine glaciers. J. Glaciol. 59, 1047–1059.

Sorg, A., Bolch, T., Stoffel, M., Solomina, O., Beniston, M., 2012. Climate change impacts on glaciers and runoff in Tien Shan (Central Asia). Nat. Clim. Change 2, 725–731.

Stahl, K., Moore, R.D., Shea, J.M., Hutchinson, D., Cannon, a. J., 2008. Coupled modelling of glacier and streamflow response to future climate scenarios. Water Resour. Res. 44, 1–13.

Stähli, M., Gustafsson, D., 2006. Long-term investigations of the snow cover in a subalpine semi-forested catchment. Hydrol. Process. 20, 411–428.

Stähli, M., Jansson, P.-E., Lundin, L.-C., 1996. Preferential water flow in a frozen soil—a two-domain model approach. Hydrol. Process. 10, 1305–1316.

Stähli, M., Jansson, P.-E., Lundin, L.-C., 1999. Soil moisture redistribution and infiltration in frozen sandy soils. Water Resour. Res. 35, 95–103.

Stähli, M., Nyberg, L., Mellander, P.-E., Jansson, P.-E., Bishop, K.H., 2001. Soil frost effects on soil water and runoff dynamics along a boreal transect: 2. Simulations. Hydrol. Process. 15, 927–941.

Stenborg, T., 1970. Delay of run-off from a glacier basin. Geogr. Ann. Ser. A, Phys. Geogr. 52, 1–30.

Storvold, R., Malnes, E., Larsen, Y., Høgda, K.A., Hamran, S.E., Müller, K., Langley, K.A., 2006. Sar remote sensing of snow parameters in Norwegian areas—current status and future perspective. J. Electromagn. Waves Appl. 20, 1751–1759.

Streletskiy, D., 2014. Permafrost degradation. In: Haeberli, W., Whiteman, C. (Eds.), Snow and Ice-Related Hazards, Risks and Disasters. Elsevier, pp. 303–344.

Surfleet, C.G., Tullos, D., 2013. Variability in effect of climate change on rain-on-snow peak flow events in a temperate climate. J. Hydrol. 479, 24–34.

Tait, A.B., 1998. Estimation of snow water equivalent using passive microwave radiation data. Remote Sens. Environ. 64, 286–291.

Taylor, S., Feng, X., Kirchner, J.W., Osterhuber, R., Klaue, B., Renshaw, C.E., 2001. Isotopic evolution of a seasonal snowpack and its melt. Water Resour. Res. 37, 759–769.

Techel, F., Pielmeier, C., 2011. Point observations of liquid water content in wet snow—investigating methodical, spatial and temporal aspects. Cryosphere 5, 405–418.

Vander Jagt, B.J., Durand, M.T., Margulis, S.A., Kim, E.J., Molotch, N.P., 2013. The effect of spatial variability on the sensitivity of passive microwave measurements to snow water equivalent. Remote Sens. Environ. 136, 163–179.

Viviroli, D., Weingartner, R., 2004. The hydrological significance of mountains: from regional to global scale. Hydrol. Earth Syst. Sci. 8, 1017–1030.

Wachter, K., 2007. The Analysis of the Danube Floods 2006 (Vienna).

Weber, M., Braun, L., Mauser, W., Prasch, M., 2010. Contribution of rain, snow-and ice melt in the upper Danube discharge today and in the future. Geogr. Fis. Dinam. Quat. 33, 221–230.

Weingartner, R., Aschwanden, H., 1992. Abflussregimes als Grundlage zur Abschätzung von Mittelwerten des Abflusses. In: Hydrologischer Atlas Der Schweiz. Federal Office for the Environment FOEN, Bern p. Tafel 5.2.

Werder, M.A., Funk, M., 2009. Dye tracing a jökulhlaup: II. Testing a jökulhlaup model against flow speeds inferred from measurements. J. Glaciol. 55, 899–908.

Zappa, M., Kan, C., 2007. Extreme heat and runoff extremes in the Swiss Alps. Nat. Hazards Earth Syst. Sci. 7, 375–389.

Zemp, M., Thibert, E., Huss, M., Stumm, D., Rolstad Denby, C., Nuth, C., Nussbaumer, S.U., Moholdt, G., Mercer, A., Mayer, C., Joerg, P.C., Jansson, P., Hynek, B., Fischer, A., Escher-Vetter, H., Elvehøy, H., Andreassen, L.M., 2013. Reanalysing glacier mass balance measurement series. Cryosphere 7, 1227–1245.